Two global datasets of daily fire emission injection heights since 2003

S. Rémy[1], A. Veira[2], R. Paugam[3], M. Sofiev[4], J.W. Kaiser[5], F. Marenco[6], S.P. Burton[7], A. Benedetti[8], R.J. Engelen[9], R. Ferrare[10], and J.W. Hair[11]

[1]Laboratoire de Météorologie Dynamique, UPMC/CNRS, Paris, France
[2]Max Planck Institute for Meteorology, Hamburg, Germany
[3]King's College, London, United Kingdom
[4]Finnish Meteorological Institute, Helsinki, Finland
[5]Max Planck Institute for Chemistry, Mainz, Germany
[6]Satellite Applications, Met Office, Exeter, United Kingdom, U.K.
[7-10-11]National Aeronautics and Space Administration, Langley Research Center, Hampton, CA, U.S.A.
[8-9]European Centre for Medium-range Weather Forecasts, Reading, U.K.

Correspondence to: S. Rémy
(samuel.remy@lmd.jussieu.fr)

Abstract.

The Global Fire Assimilation System (GFAS) assimilates Fire Radiative Power (FRP) observations from satellite-based sensors to produce daily estimates of biomass burning emissions. It has been extended to include information about injection heights derived from fire observations and meteorological information from the operational weather forecasts of ECMWF.

Injection heights are provided by two distinct methods: the Integrated monitoring and modelling System For wildland Fires (IS4FIRES) parameterization and the one-dimensional Plume Rise Model (PRM). A global database of daily biomass burning emissions and injection heights at 0.1° resolution has been produced for 2003-2015 and is continuouly extended in near-real-time with the operational GFAS service of the Copernicus Atmospheric Monitoring Service (CAMS).

In this study, the two injection height datasets were compared against the new MPHP2 (MISR Plume Height Project 2) satellite-based plume height retrievals. The IS4FIRES parameterization showed a better overall agreement against observations, while the PRM was better at capturing the variability of injection heights. The performance of both parameterizations is also dependent on the type of vegetation.

Furthermore, the use of biomass burning emission heights from GFAS in atmospheric composition forecasts was assessed in two case studies: the South AMerican Biomass Burning Analysis (SAMBBA) campaign which took place in September 2012 in Brazil, and a series of large fire events in the Western U.S. in August 2013. For these case studies, forecasts of biomass burning aerosol species by the Composition-Integrated Forecasting System (C-IFS) of CAMS were found to better reproduce the observed vertical distribution when using PRM injection heights from GFAS as compared to aerosols emissions being prescribed at the surface.

The globally available GFAS injection heights introduced and evaluated in this study provide a comprehensive dataset for future fire and atmospheric composition modelling studies.

1 Introduction

Vegetation fires are responsible for the release of large quantities of trace gases and aerosols into the atmosphere (Andreae and Merlet , 2001 and Van der Werf et al., 2010). Each year, around 3 million square kilometers are burnt worldwide (Giglio et al., 2010) by landscape fires ignited by natural or anthropogenic causes. A wide range of atmospheric processes are affected by fire emissions, including radiative transfer, turbulent diffusion, cloud microphysics and atmospheric chemistry (Twomey, 1977; Heald et al., 2014; Veira et al., 2015b among others). Fires cause large emissions of particulate matter; they have been estimated at 2-11 Tg of black carbon per year and 18-77 Tg of organic carbon per year (Bond et al., 2013, and references therein). This can result in acute air quality problems, such as in Singapore in June 2013 for example when the air quality index reached record values because of smokes from fires in nearby Sumatra.

Several global fire emission database have been developed in the recent years: FLAMBE (Fire Locating and Modeling of Burning Emissions), GFED (Global Fire Emissions Database), FINN (Fire INventory from NCAR), QFED (Quick Fire Emission Dataset), IS4FIRES and GFAS (Reid et al., 2009; Van der Werf et al., 2010 and Giglio et al., 2013; Wiedinmyer et al., 2011; Darmenov and da Silva, 2013;Sofiev et al., 2009; Kaiser et al., 2012 respectively). All of these products rely on satellite observations of Fire Radiative Power (FRP), hot spots or burnt area because they alone provide sufficient spatial coverage and temporal sampling frequency (Giglio et al., 2006; Kaiser et al., 2012).

When a fire is in the flaming combustion stage, the intense heat from the burning vegetation creates a rising plume which interacts with the ambient atmosphere and transports the fire emissions vertically (Freitas et al., 2006; Paugam et al., 2015a). Because of this fire-induced convection, biomass burning is one of the few processes that emit large quantities of aerosols and trace gases well above the Planetary Boundary Layer (PBL), sometimes even reaching the upper troposphere/lower strato-sphere ((Andreae et al., 2004); Fromm et al., 2005; Dahlkötter et al., 2013). Using observations from the Multi-angle Imaging SpectroRadiometer (MISR) instrument onboard Terra, Kahn et al. (2008) estimated that 5 to 18% of fires that occurred over Alaska and Canadian Yukon in 2004 released smoke constituents above the PBL. A five year record of MISR observations by Valmartin et al. (2010) found a similar figure. Sofiev et al. (2012), using an injection height parameterization, found that 15% of fire plumes reached the free troposphere. Fires in the smoldering stage can also produce a significant amount of smoke, which is mostly released just above the surface, e.g. Tosca et al. (2011).

Fire emission height, i.e. the height at which the fire releases emissions into the atmosphere, has been identified as a crucial parameter to influence the forecasts of the life cycle of biomass burning aerosols. In particular, whether smoke constituents are released below or above the top of the PBL will have profound consequences on their transport, deposition and life cycle. There are significant uncertainties in the vertical distribution of aerosols in global models (Textor et al., 2006), which has an impact in estimating the magnitude of the direct radiative forcing of aerosols (Choi and Chung, 2014).

The height at which smoke constituents are released depends on the atmospheric environment and on the intensity of the updraft generated by the fire, which itself depends on a variety of parameters (Kahn et al., 2007); foremost among them are the sensible heat flux and the size of the fire. The ambient atmosphere has a twofold impact on the vertical transport in a fire plume: the thermal stratification acts more or less strongly against the buoyancy triggered by the sensible heat released by

the fire. Because the environment is cooler than the plume, water vapour condensation and latent heat release occur, with the formation of pyro-cumulus and/or -cumulonimbus (Fromm et al., 2010): this can accelerate the vertical transport in the smoke plume. The vertical wind-shear also impacts both the vertical and the horizontal development of the plume.

Several theories and models describing the dynamics of plume rise have been developed. The algorithms available today are summed up in Paugam et al. (2015a) and Veira et al. (2015a). They can be divided into two families: semi-empirical models (Achtemeier et al., 2011 and Sofiev et al., 2012 for example) and numerical one-dimensional Plume Rise Models (PRM) such as the one developed by Latham (1994) and further refined by Freitas et al. (2007) and others. All of these models use as input atmospheric profiles of meteorological parameters together with satellite information on fire size and/or activity. Their output is either an injection height or a full smoke detrainment profile.

The Global Fire Assimilation System (GFAS) of the EU-funded operational Copernicus Atmosphere Monitoring Service (CAMS Hollingsworth et al., 2008; Flemming et al., 2015) has recently been updated to include injection height information based on the IS4FIRES parameterization (Sofiev et al., 2012) and a PRM (Freitas et al., 2007). These new products have been calculated for the time period since 2003 and are being continued as an operational near-real time service on a daily basis. They are freely available online at http://apps.ecmwf.int/datasets/data/cams-gfas.

In this study, we describe the GFAS update in detail, validate the new injection height information against MISR observations, and demonstrate its positive impact on atmospheric aerosol simulations in two case studies. In Section 2, we present the IS4FIRES and PRM algorithms as well as the verification dataset from MPHP2. The C-IFS model is also introduced in this section. Section 3 details how the injection heights algorithms were embedded in GFAS. Section 4 shows the two injection height datasets and their validation against the MPHP2 dataset. Section 5 presents two applications of injection heights from GFAS using the C-IFS atmospheric composition model for two field campaigns in South America and the US. The manuscript then summarises our conclusions and provides details on the recent updates of the PRM in Annex A.

2 Methodology: models and data

A model that aims to predict the evolution of a smoke plume with time typically uses two kind of inputs: information about the environment (temperature and wind profiles), and about the fire (Fire Radiative Power and fire area). Figure 1 shows a schematic sketch of how a fire plume is modeled using these inputs and of the various injection height parameters that are used in this study. Plume detrainment is the quantity of smoke that is shed by the plume into the environment. The various injection height parameters. Detrainment is used to define the mean height of maximum injection, which corresponds to the average of the plume heights at which detrainment exceeds half of the maximum value.

2.1 Plume Rise Model (PRM)

The PRM comes in two versions: v0, used in the work of Valmartin et al. (2012) and Strada et al. (2013) and described in detail in Freitas et al. (2007) and Freitas et al. (2010), and v2 which is presented in Paugam et al. (2015b). The modifications brought by Paugam et al. (2015b) concern mass conservation and the entrainment scheme; they are summarized in Annex A.

In this work, PRM v2 is used and the term "PRM" will denote this particular version. The Plume Rise Model consists of a 1-D cloud-resolving model, forced at its base by satellite-derived fire parameters: Convective Heat Flux (CHF), and Active Fire area (AF-area). To account for possible condensation and formation of pyro-cumulus, the PRM also includes a bulk microphysical scheme based on Kessler (1969). Four prognostic variables: vertical velocity; temperature; horizontal plume velocity and the radius of the plume are forecasted by the model. These 4 variables are governed by equations based on the vertical motion and mass conservation equations as well as the first thermodynamic law (Freitas et al., 2007).

The PRM is run using a 100 m resolution vertical grid, reaching a maximum height of 20 km. The time step is adaptive, computed to respect the Courant-Friedrich-Levy numerical stability criterion, with an upper limit of 5 seconds (Freitas et al., 2007). The ambient atmospheric profiles of temperature, wind and specific humidity are taken from 3-hourly European Centre for Medium Range Forecasts (ECMWF) data.

Besides the atmospheric profiles, the main inputs of the PRM are Convective Heat Flux (CHF) and Active Fire (AF)-area. CHF is defined as :

$$CHF = \beta.FRP \tag{1}$$

Where β is a scaling factor (see Annex A for the values of the parameters of the PRMv2). The Active Fire area is estimated from MODIS observations in the mid- and thermal- infrared channels using the Dozier algorithm (Dozier, 1981)) on clusters of contiguous active fire pixels. Injection heights are computed only for fires with an area above 1 ha, and a MODIS sub-pixel effective temperature above 600K, to prevent taking into account smoldering fires. There is no output for these fires for which most of the emissions take place close to the surface.

2.2 IS4FIRES

The semi-empirical IS4FIRES parameterization is detailed in Sofiev et al. (2012). Injection height is estimated as a function of the PBL height, the Brunt-Väisälä frequency of the free troposphere and the FRP of a fire. In our implementation, the PBL height is provided by the operational ECMWF model, which uses the Troen and Mahrt (1986) diagnostic: PBL height is defined as the level where the bulk Richardson number, based on the difference between quantities at that level and the lowest model level, reaches the critical value 0.25. Evaluation of this product against satellite retrievals (Palm et al., 2005) showed that the diagnostic often underestimates the PBL height by a few hundred meters but shows a good correlation with observations. In this work the two-step version of the IS4FIRES algorithm is used.

IS4FIRES was further refined by Kukkonen et al. (2014) and Veira et al. (2015a). Kukkonen et al. (2014) improved the results of the algorithm when replacing the Brunt-Väisälä frequency of the free troposphere by the inversion layer Brunt-Väisälä frequency in case of stable nocturnal boundary layer. Since our proposed implementation will use a daily FRP product that is based on day-time satellite observations from MODIS, this improvement was not tested and its impact would probably not be significant.

2.3 MISR plume heights: MPHP2

The MPHP plume height dataset is a combination of the MISR smoke aerosol and the MODIS MOD14 thermal anomaly products. The MISR instrument is hosted by Terra and consists of 9 cameras that are viewing the Earth at different angles, in four spectral channels in the visible and near-infrared spectrum. The height of the smoke plume is retrieved stereoscopically by measuring the parallax observed between pairs of camera images out of a total of 9 cameras (Nelson et al., 2013). A correction is applied to account for the movement of the plume, using an externally provided wind direction. The latest release of the MPHP (April 2012) includes data of wildfire smoke plumes in North and South America, Eurasia, Africa and Southeast Asia, observed between 2001 and 2009. For more detailed information, see the official product description at http://www-misr.jpl.nasa.gov/getData/accessData/MisrMinxPlumes/. As stated in the MPHP data quality statement, important biases are introduced by pyro-cumulus clouds which hide below-cloud fire activity (Kahn et al., 2008), by errors in the digitization of the plumes and by large uncertainties in the MODIS fire pixels.

The MPHP2 dataset that was released in July 2015 is using a new version of the satellite retrieval software, with the addition of a blue-band height retrieval to the existing red-band retrieval, which should enhance the quality of the dataset for optically thin plumes over bright surfaces. The MISR conventional red-band retrieval of height for optically thin smoke over relatively bright terrain is frequently unsuccessful and may under-estimate smoke height. Height retrievals for many plumes in the MPHP2 dataset used the blue-band retrieval, resulting in a significant increase in the number of successful plume retrievals. The MPHP2 dataset includes over 32000 fire plumes for the year 2008. When excluding plumes of poor retrieval quality, the MPHP2 dataset provides 13454 injection heights which we will use to validate the injection heights from the two algorithms embedded into GFAS.

According to the official MPHP product description as well as Kahn et al. (2008) and Nelson et al. (2013), an observational plume height accuracy of about 200 m can be assumed in good conditions. In the absence of a different prescription for the new dataset, we will use the same value for the MPHP2 dataset.

2.4 The C-IFS forecasting system

The C-IFS global atmospheric composition model is an assimilation and forecasting system for monitoring aerosols, greenhouse gases and reactive gases, using satellite observations and a combination of global and regional models (Hollingsworth et al., 2008; Peuch and Engelen, 2012) operated by CAMS. The meteorological component of C-IFS is based on the ECWMF operational model, the Integrated Forecast System (IFS). The trace gases component of C-IFS is described in Flemming et al. (2015).

Aerosols are forecasted within the C-IFS global system by a forward model (Morcrette et al., 2009, based on earlier work by Reddy et al., 2005 and Boucher et al., 2002) that uses five species: dust, sea-salt, black carbon, organic matter and sulfates. GFAS provides the biomass burning emissions of black carbon, organic matter and sulfates. In this chapter the sum of Black Carbon (BC) and Organic Matter (OM) is hereafter denoted as "biomass burning aerosols". Sulphates were excluded because for there are many other important sources for this species besides fires. C-IFS provides and uses aerosol analysis by

assimilating total Aerosol Optical Depth (AOD) observations from MODIS in a 4D-Var assimilation algorithm, as described in Benedetti et al. (2009).

The prognostic variables of C-IFS are mass mixing ratios. Extinction and AOD at 17 wavelengths (see table 1 of Morcrette et al., 2009) are diagnosed using a standard Mie scattering algorithm (Ackerman and Toon, 1981) using an external mixing assumption. Absorption and scattering coefficients for organic and black carbon, and sulphate were adapted from those in the LOA/LMD-Z model. For more information, please refer to Table 2 and Figure 1 of Reddy et al. (2005).

3 Integration of IS4FIRES and PRM in GFAS

3.1 Overview of the Global Fire Assimilation System (GFAS)

CAMS provides global analysis and forecasts of atmospheric composition, alongside European air quality forecasts (Hollingsworth et al., 2008) using the C-IFS model (Morcrette et al., 2009; Benedetti et al., 2009; Peuch and Engelen, 2012 and Flemming et al., 2015). In order to provide this forecasting system with accurate estimates of aerosol, reactive gases and greenhouse gas emissions from biomass burning, GFAS (Kaiser et al., 2009, 2012) uses satellite measurements of fire radiative power (FRP) to estimate fire emissions. GFAS is operated operationally within the CAMS project and provides daily estimates of FRP, dry matter burnt and biomass burning emissions of 41 species.

GFAS grids and averages FRP observations from the MODIS instrument onboard the National Aeronautics and Space Administration (NASA) Terra and Aqua satellites. The gridded data from the two satellites are then merged to produce global daily averaged FRP fields with 0.1 ° resolution. Analyses of daily averaged FRP are constructed by assimilating these merged daily averaged FRP observations. The assimilation step consists of a simple Kalman filter used with a persistence model. The objective of the data assimilation step is to correct for gaps in the observations, caused mainly by cloudy conditions (sometimes caused by pyro-cumulus or -cumulonimbus). Spurious FRP observations of volcanoes, gas flares and other industrial activity are masked using a fixed spurious signal mask.

Correlations between FRP and fuel consumption with fire emission were found in several contexts: Wooster et al. (2005) demonstrated this for fuel consumption in laboratory studies, Ichoku and Kaufman (2005) documented it for aerosol emission observed by satellite, and Heil et al. (2010) found strong, but biome-specific, correlations between FRP and the dry matter combustion rate of GFEDv3.1 (Van der Werf et al., 2010). This allowed the derivation of conversion factors for eight land covers classes that link GFAS FRP to GFED dry matter combustion rate, and subsequently the estimation of global dry matter burnt fields with GFAS. Emission factors following Andreae and Merlet (2001) and updates are then used to estimate the emissions of 41 species from the dry matter burnt.

The GFAS emission inventory covers the period from 1 January 2003 to present. It has been recently extended to early 2000 (Remy and Kaiser, 2014) using bias-corrected observations from MODIS onboard Terra only. The output from GFAS is validated regularly in the framework of the CAMS project (e.g. Andela et al., 2013).

3.2 Integration of the injection height algorithms into GFAS

The output of the IS4FIRES parameterization is a single parameter: injection height, which makes it easy to assimilate once gridded and averaged. The output of the PRM is a whole detrainment profile, which would be too costly to assimilate. It was decided instead to derive the most useful parameters from this profile and then to regrid and assimilate them. These parameters consist of the top and the bottom of the plume, and of the mean height of maximum injection, i.e. the average of the PRM levels for which detrainment is equal or above half of maximum detrainment.

The clustering algorithm of the PRM was used to produce clusters of contiguous MODIS fire pixels. The PRM was run with accumulated FRP of each fire cluster as an input while the maximum FRP of each cluster was used as input to IS4FIRES, so as to use inputs that are similar to Sofiev et al. (2012).

The output of the PRM is very dependent on the stability of the atmosphere. One possible drawback is that in some cases, the impact of the fire forcing at the base of the 1D column of the PRM becomes negligible as compared to the impact of the atmospheric environment. In that case, the injection profiles produced by the PRM are only representative for the convective updrafts in the environment, but not for the pyrogenic convection. To prevent this, the PRM is run twice, once with no fire forcing, and another time with the fire forcing. Only the fire clusters for which the mean height of maximum injection provided by the PRM forced by the fire is larger than the one provided by the PRM not forced by the fire are kept. This particular criterion removes around 10 % of active fire clusters.

The two injection height algorithms provide four parameters, for each 5 mn MODIS granule: three for the PRM (mean height of maximum injection, height of the top of the plume and of the bottom of plume), and one for IS4FIRES. These parameters must first be gridded onto the 0.1 x 0.1 ° GFAS grid. To achieve that, the number and coordinates of all the MODIS pixels that constitute the fire clusters are kept. Each GFAS grid cell containing at least one pixel of a given fire cluster is then associated with the values of the four injection heights of this fire cluster. In the case where a GFAS grid cell contains pixels from two or more distinct fire clusters, the maximum value from the fire clusters is assigned to the GFAS grid cell. Maximum FRP from each fire clusters is also gridded in the same way.

In GFAS, the time averaging of the 5 mn global gridded FRP into hourly and daily global gridded FRP uses the fraction of satellite observed area as a weight. For the injection height parameters it was decided to use the gridded maximum FRP as a weight in order to privilege injection heights associated with the most active fires. This means that the resulting product is more representative of the diurnal maximum of fire intensity. The rationale behind this choice is that several studies showed that most of emissions from biomass-burning occur within a few hours of a peak time, typically during the early afternoon (Andela et al., 2015, Freeborn et al., 2009, Freeborn et al., 2011, Roberts et al., 2009). The daily gridded fields of the four injection height parameters are then assimilated alongside FRP in the data assimilation step of GFAS.

There are many GFAS grid cells with non-null FRP and biomass burning emissions with null injection heights because the PRM does not always produce a detrainment profile for a given fire cluster (depending on fire temperature, fire size and the output from the non-forced PRM mentioned above). In most cases, these grid cells correspond to fires in the smoldering stage for which most of the plume material is emitted close to the surface. For these grid cells, it is recommended for atmospheric

composition applications to release biomass burning emissions at the surface. In all, only 33 to 35% of GFAS grid cells with positive fire emissions also have positive injection height parameters. They correspond to fires in the flaming stage.

4   Results and validation

In this section, the output of the two algorithms embedded into GFAS is evaluated: injection height for IS4FIRES and mean
5   height of maximum injection for the PRM (see Figure 1 for a sketch), ie the average of the PRM levels for which detrainment is above half of maximum detrainment. The injection height from IS4FIRES correspond to the top of the plume, as do the MPHP2 retrievals. It was chosen however to use the mean height of maximum injection as the reference output from the PRM because the plume top often appeared to be much higher than height of maximum injection, which is not often the case for real fires. For the sake of simplicity, the mean height of maximum injection from the PRM will also be called "injection height".

10   ### 4.1   Comparison of the raw output of the two algorithms

Figure 3 shows density plots of the injection height provided by the IS4FIRES parameterization against the boundary layer height diagnostic from the operational ECMWF model, for global Terra and Aqua observations and for the 1/6/2013 to 1/8/2013 period. The injection heights are neatly separated into two distinct subsets: one below the PBL height, with a large variability, and another just above PBL height with low variability. The two subsets are clearly a result of the two steps of the algorithm,
15   with the second step being applied only to plumes that are rising higher than the PBL height. However, it is apparent from this plot that IS4FIRES encounters difficulties in providing injection heights that are significantly above PBL height.

The same plot also shows density plots of the mean height of maximum injection provided by the PRM against the boundary layer height diagnostic from the operational ECMWF model, for global Terra and Aqua observations and for the 1/6/2013 to 1/8/2013 period. The impact of the thermal stratification of the atmosphere is apparent: for most of the fire plumes, maximum
20   detrainment occurs just under the top of the PBL, where a temperature inversion sometimes occurs and may block the vertical development of fire plumes. Maximum injection occurs higher with Aqua observations than with Terra. The Terra overpass time at the Equator is around 10:30 local solar time in its descending mode and 22:30 local solar time in its ascending mode. The Aqua overpass times at the Equator are around 13:30 (resp. 01:30) local solar time in ascending (resp. descending) mode.

The different values for maximum injection obtained with Aqua and Terra observations show that the two methods reproduce
25   the maximum of the diurnal cycle of fire activity during the early afternoon well. With Terra observations, a number of cases with a very stable PBL give very low maximum injection heights; this is more marked for the PRM. With Aqua, the number of such cases is smaller.

4.2   Comparison of the two injection height datasets

The extended version of GFAS has been run from 1 Jan 2003 to 1 Jan 2015. The resulting injection height datasets from
30   IS4FIRES and mean height of maximum injection from the PRM are evaluated in this section.

The average values of the mean height of maximum injection and of the plume top, from the PRM component of GFAS, and of the injection height from the IS4FIRES component of GFAS are presented in Figure 4. For the sake of simplicity, these two components will be named as "PRM" and "IS4FIRES" respectively. Over most of regions except Siberia, Russia and Ukraine, the injection height from the PRM (i.e. the mean height of maximum injection) is above the injection height from IS4FIRES. The main biomass burning regions: Brazil, Africa North and South of the Equator, SE Asia and Australia, are prominent on all the plots, with injection heights that are higher than other regions such as China, India and Central America. The two algorithms estimate the higher injection heights over Central Australia, for a limited number of fires however.

The output from IS4FIRES and PRM are compared in table 2 for the regions of interest defined in Kaiser et al. (2012) (shown in Figure 1). In addition to the average, the 1st, 5th (median) and 9th deciles are given for all regions. The mean of the PBL height diagnostic from the ECMWF model for grid points that include fires only is also given. The average of the PRM injection heights is globally approximately 150 m higher than the IS4FIRES injection height. The regional variability is high, with Tropical Asia and Europe showing the lowest injection heights on average for the two algorithms, and Australia the highest. The intra-regional variability is much larger for the PRM than for IS4FIRES injection heights: the lowest plumes are much lower with the PRM, and the highest plume much higher as well. This was also shown by Paugam et al. (2015b) : the PRM seems more able to estimate the higher injection heights. The 9th decile is on average 650 m higher for the PRM as compared to IS4FIRES. Maximum values of injection heights can reach 7 or 8 km on occasion with the PRM while they very seldom reach 4 km with IS4FIRES.

This table also confirms that there is a significant statistical link between PBL height and injection heights, more marked with the PRM. The PBL height diagnostic from ECMWF for grid cells with fires show low values for Tropical Asia. This is probably because most of fires occur quite close to the sea in this region, which comprises mainly Indonesia. The spatial interpolation may thus include PBL height values from over the sea, which are lower than over land because of lower day-time heat flux from the surface. Besides this region, the regions that display the lowest and the highest averages injection heights with the PRM are also the regions with lowest and highest PBL heights at grid cells with fires. Comparing the 9th decile with PBL height shows that for all regions, the 9th decile of PRM injection heights is significantly above the PBL height diagnostic. This means that with the PRM and for all regions, more than 10% of fires release their constituents mainly in the free atmosphere. For the IS4FIRES parameterization, this is true only for some specific regions: Australia, South America, North Asia and Tropical Asia. For the most active biomass burning region globally, Africa, North and South of the Equator, the difference between the PRM and IS4FIRES injection heights is significant in terms of the number of fires that release their emissions above the PBL.

This greater variability of the PRM as compared to IS4FIRES is also apparent in Figure 5, which shows global and regional density plots of median injection heights from the PRM versus IS4FIRES. The linear fit between the two sets indicates that for all regions, the extreme values are more extreme with the PRM. For some regions such as Europe and North Hemisphere Africa, the median injection height from the PRM is below 500 m in many cases. For these two regions, the mean and median of injection heights are significantly lower with the PRM than with IS4FIRES; which shows that this has a strong impact

on regional statistics. This plot also highlights the regional variability, which is more marked for the PRM as compared to IS4FIRES injection heights.

4.3 Validation against MISR observations of plume top heights

In this section, the newly computed injection heights are compared against the MPHP2 dataset of injection heights derived from MISR observations for each GFAS grid cell in which both MPHP2 observations and GFAS injection heights are available. By taking into account only the plumes with good and fair retrieval quality, the verification dataset is composed of 13454 injection heights. When collocating these observations against the non-null injection heights computed from Terra-based fire observations in GFAS, the sample size is reduced to 4182, or 31% of the initial verification dataset.

4.3.1 Global scores

The global injection height distribution of the MPHP2, PRM and IS4FIRES injection heights is shown in Figure 6. The values are all for fires for which a MPHP2 injection height estimate of fair or good quality is available. The IS4FIRES injection heights are more often closer to the MPHP2 values, especially between 800 and 2000m, which represents the majority of cases. The PRM shows a significant overestimation of the frequency of injection heights below 500 m; this is especially apparent for very low injection heights (200 m). These very low values from the PRM should clearly be disregarded. The IS4FIRES parameterization on the other hand underestimates the number of plumes with injection heights below 1000 m. For injection heights above 2500 m, i.e. in the upper tail of the vertical distribution, the PRM gives a frequency that is closer to observations. These plumes constitute a minority of observed plumes, but they are particularly important in terms of atmospheric composition they are particularly large and they are subject to long-range transport in the free troposphere.

Figure 7 present global density plots of MPHP2 injection heights versus IS4FIRES and PRM injection heights from GFAS, and the associated statistical scores are detailed in Table 3. The IS4FIRES injection heights show a small positive bias; this bias is especially marked for observed injection heights that are below 1000 m. On the other hand, for MPHP2 values above 3 km, the IS4FIRES injection heights are often significantly underestimated, by more than 1000 m in a number of cases. This shortfall of the IS4FIRES parameterization was already noted in Sofiev et al. (2012) and Veira et al. (2015a). For MPHP2 plumes between 1000 and 2000 m, which represent a majority of observations, the IS4FIRES injection heights are often within 500 m of the observations.

The larger variability and the more important positive bias of the PRM injection heights are also apparent in Figure 7 and table 3. A significant number of plumes are forecasted with injection heights at 200 m, while observation for these plumes range from 500 to 2500 m. This brings a small degradation of the RMSE of the PRM, which is nearly two times larger than the RMSE of IS4FIRES injection heights. The PRM is more able to estimate larger injection heights as compare to the IS4FIRES parameterization, and a larger fraction of the observed injection heights above 3 km is well forecasted. However, the majority of injection heights estimated by the PRM to be larger than 3 km correspond to MPHP2 values well below 2500 m. This is consistent with the findings of Valmartin et al. (2012) who found, with an earlier version of the PRM, that 44% of the plumes are incorrectly estimated to reach the free troposphere.

4.3.2 Regional scores

Global and regional scores are summed up in table 3. The proportion of estimated plumes that fall within 500 m of the observations is also displayed. Globally and for all regions, 55 to 65% of injection heights from IS4FIRES fall within 500 m of the observations against 40 to 50% for PRM injection heights. Correlation between estimations and observations is also higher for IS4FIRES's injection heights, with values ranging from 0.4 to 0.55 for the correlation coefficient, against 0.3 to 0.4 for PRM injection heights. The figures for IS4FIRES injection heights are close to the results of Sofiev et al. (2012); the fraction of plumes that fall within 500 m of the observations being a bit lower.

The lower scores of the PRM injection heights are associated with a much larger RMSE and bias, globally and for all regions. The two algorithms show a correlation in both bias and RMSE: The regions with maximum and minimum bias and error are the same for both algorithms, with larger values for the PRM. This is because the errors are larger for higher injection heights in both calculations.

4.3.3 Scores per biome type

The MPHP2 dataset also include the MODIS land cover type product following the International Geosphere-Biosphere Program (IGBP) classification (Channan et al. , 2014). Scores for each IGBP biome type are shown in table 4. They help understand the strengths and weaknesses of each algorithm. The PRM shows a large bias of 664m for evergreen broad-leaf forests, and a bias of more than 350 m for savannas and woody savannas. This could come from the fact that the parameters of the PRM were derived by optimization against a small number of plumes in North America (Paugam et al., 2015b), which may not at all include plumes over this kind of land cover. For these biome types, which represent more than half of all the MPHP2 dataset, the RMSE is also very large for the PRM.

The RMSE and bias are both significantly lower for IS4FIRES injection heights, for all biome types. The variability depending on the biome type is also lower for IS4FIRES. For both injection heights, the best results are achieved on fires occurring in deciduous needle-leaf forests areas, i.e. boreal fires. For the PRM, optimization of the parameters was done on fires occurring just over such land covers.

4.4 Discussion

There are three sources of errors in the injection height estimates that were assessed in this study (besides possible errors on the verification dataset):

– Uncertainties on the MODIS satellite products that are used as input,

– Uncertainties on the ECMWF profiles that are used to provide information on the environment,

– And finally, simplifications and/or processes not represented in the algorithms.

These three sources of errors all play a role in the scores. MODIS FRP is often underestimated (Kahn et al., 2008; Schroeder et al., 2014). This underestimation seems to be more significant for large fires, because of the opacity effect whereby the smoke

hinders the remote detection of thermal anomalies at the surface. Veira et al. (2015a) improved scores of another version of IS4FIRES against the MPHP dataset by applying an empirical FRP correction for plumes higher than a threshold height. This hasn't been tried yet in this study; however this modification will probably increase the small positive bias against MPHP2 injection heights of the IS4FIRES injection heights. Tests were carried out using the accumulated FRP of the fire cluster instead

5   of the cluster maximum FRP as an input for the IS4FIRES parameterization. This didn't have much impact on the output and the scores, despite a much larger input value for FRP of large fires.

Using additional satellite products, especially from geostationary satellites, can only improve the quality of the injection heights and of the GFAS products as a whole. This would also allow to describe the diurnal cycle of fires and injection heights. Work is going on to combine the accuracy of low orbit observations with the better time resolution of geostationary products

10   in GFAS (Andela et al., 2015).

The two algorithms are very dependent on the atmospheric profiles provided by the ECWMF. The diagnosed PBL height is of special important since plumes often reach the top of the PBL without breaking through to the free troposphere. Even if the ECMWF diagnostic appears to be of good quality generally (see the studies of Palm et al. (2005) and Flentje (2014)), possible errors will have a large impact on injection height estimates from both algorithms. In particular, given the strong

15   correlation between the PRM injection height and PBL height (see figure 3, it is possible that the numerous cases where the PRM estimates very small injection heights (200-300 m) while the MPHP2 dataset gives values from 1000 to 2000 m correspond to cases where the PBL height according to ECMWF was underestimated. In some cases, especially over Indonesia, some land-sea mask representativity issues arose for the ECMWF PBL height and environment profiles, caused by the coarse 1x1° grid that was used. The bad scores of the PRM over Indonesia were improved when using a better resolution for the

20   atmospheric environment. The extra computing cost of increasing the resolution of the environment is however too great to consider this option for running GFAS in Near Real Time (NRT) mode or to produce climatology. Strada et al. (2013) found a great sensitivity of the PRM to ambient wind and humidity. In this implementation, the atmospheric stability was found to be have the most impact on the output of the PRM.

Also, the fact that the PBL height diagnosis from ECMWF was used in IS4FIRES instead of the PBL height formulations

25   used in Sofiev et al. (2012) and Sofiev et al. (2013) could be a source of error for this algorithm.

The PRM is a much more complex algorithm than IS4FIRES, using an estimate of fire size as an additional input, and taking into account wind drag, plume microphysics, entrainment and detrainment in its parameterization. This increased complexity makes it more able to estimate large injection heights; however it also means that it is less robust than IS4FIRES in the sense that it is subject to more sources of uncertainty, notably on fire size. The fact that 6 parameters (see Annex A) in its system

30   of equations were fitted from a small number of plumes may have degraded its results, especially for the land cover types that were not taken into account in Paugam et al. (2015b). The PRM was also shown to be very sensitive to entrainment (Valmartin et al., 2012), for which there is very little information available.

Additionally for the PRM, the fact that a whole detrainment profile is translated into only 3 parameters (mean height of maximum of injection, top of the plume, bottom of the plume) is an additional source of error.

5 Use of GFAS injection heights in C-IFS

This chapter presents two case studies for the use of assimilated injection heights from GFAS in C-IFS: the SAMBBA campaign which took place in September 2012 in Brazil, and a series of large fire events in the Western U.S. in August 2013. It should be noted that the comparisons between observation and model in this section can only be of a qualitative nature. Due to the large range of possible modeling errors (regarding sources, atmospheric transport, aerosol processes, etc.), the use on injection heights is only one of the numerous factors that impacts on the simulated biomass-burning aerosol extinction.

C-IFS used to emit biomass burning aerosols at the surface. The model was modified to allow biomass burning emissions to be injected at the level of the PRM mean height of maximum injection from GFAS. A criterion on the PBL height diagnostic was added to prevent emitting biomass burning aerosols too high at night: the injection height provided by the PRM is used only when PBL height is above 500 m. The PRM was chosen for a first implementation because it appears to estimate better high injection heights, associated with large fires, which have a more important impact on atmospheric composition. The IS4FIRES injection heights will be used in an upcoming test, since they show better scores overall in comparison with the MPHP2 dataset.

When used in C-IFS, the GFAS emissions of biomass burning aerosols are scaled by a factor of 3.4. This value was estimated by Kaiser et al. (2012) by comparing simulations with and without data assimilation, both using GFAS for biomass-burning sources. The scaling factor was recomputed using the same method but for Organic Matter (OM) and Black Carbon (BC) separately (rather than for the sum of these two) using one year C-IFS runs with and without data assimilation, with biomass-burning aerosol emissions prescribed at the surface and at the mean height of maximum injection provided by the PRM. The result is shown in figure 8. The use of injection heights has an overall small impact on OM and BC optical depths simulated by C-IFS; however it is more significant when large fire events occur, such as in the summer 2013. The optical depths of both OM and BC are higher when emissions are at an altitude rather than at the surface. This can be explained by the fact that aerosols emitted at the surface are immediately subjected to dry deposition, which is not the case when they are emitted higher up. This increases residency time for aerosols that are emitted at an altitude as compared to aerosols emitted at the surface.

For OM, the scaling factor with emissions prescribed at the surface varies from 2.7 to 5, the smaller values corresponding to large fire events. The global average is 3.2. For BC, the same scaling factor varies from 4.9 to 7, with a 6.1 average. With emissions at the mean height of maximum injection, the global average for OM and BC scaling factors are 3.0 and 5.9 respectively, to be compared against values of 3.2 and 6.1 when biomass burning emissions are prescribed at the surface.

These results are applicable only to GFAS biomass burning emissions used in the C-IFS model: other models also use scaling factor for biomass-burning emissions, but their values are different: 1.7 for the Met Office Unified Model limited area model configuration over South America that was used used for the SAMBBA campaign, which also made use of GFAS emissions (Kolusu et al., 2015; Marenco et al., 2016); GEOS-5 uses scaling factors for GFED emissions of 1.8 for savanna and grassland, 2.5 for tropical forest and 4.5 for extra-tropical forest (Colarco, 2011).

5.1 SAMBBA field campaign

The South AMerican Biomass Burning Analysis (SAMBBA) campaign was an intensive field campaign which took place in September-October 2012 in Brazil, aimed at investigating the properties of biomass burning aerosols over the Amazon basin. The main biomass burning season occurs there during July-October, when deforestation fires and agricultural burning are frequent. Marenco et al. (2016) analyzed lidar observations of smoke aerosols from six flights of the Facility for Airborne Atmospheric Measurements (FAAM) BAe-146 research aircraft. The ground tracks of the considered flights are shown in Figure 9 and table 5, reproduced from Marenco et al. (2016). The flights took place during intense biomass burning episodes in the East of the Amazon Basin. Figure 9 shows the PRM top of the plume and mean height of maximum injection from GFAS for the 16 to 29 September 2012 period. The first period, 16-22 September, is characterized by intense fires, with mean heights of maximum injection often reaching more than 4 km between between 10 and 15°S and 45-55 °W, and top of the plume estimated at more than 5 km for some fires in this box.

The cross-sections of the aerosol extinction coefficient from the lidar observations for the six considered research flights are presented in Figure 10. All of the six flights show enhanced extinction that has been ascribed to biomass burning, with smoke layers lying at altitudes varying from 2 to 4 km. Extinction profiles from several flights (B733 and B741 especially) show two or more distinct aerosol layers, which may originate from distinct fires. The elevation of the observed aerosol layers is close to the mean heights of maximum injection provided by GFAS in the region, i.e. between 3 and 4 km generally.

As detailed in Marenco et al. (2016), the observed profiles of aerosol extinction were compared against model predictions from the Met Office Unified Model (MetUM) and C-IFS. The results from the MetUM are presented and analyzed in Marenco et al. (2016). Figure 11 shows the simulated extinction profiles from C-IFS along the flight track, with biomass burning aerosols injected at the surface and at the PRM mean height of maximum injection provided by GFAS.

Except for flight B741, the aerosol extinction is larger when the biomass burning aerosol are injected at an altitude, for the same reasons as explained previously.

Comparing to observations, using the PRM injection height from GFAS seems to bring an improvement in the forecasts of the aerosol extinction profiles for flights B742, B743 and also B746. For these flights, the observed layers of aerosols at 4 km (B742), 2 km (B743) and 2.5 km (B746) are better represented when using injection heights while they are either nearly absent (B742) or underestimated (B743 and B744) when biomass burning aerosols are emitted at the surface. For flight B742, the modified model is able to forecast the two aerosol layers that were observed. For flights B734 and B741, there is no discernible improvement or degradation while for flight B733, the use of injection heights increased the simulated aerosol burden in the smoke plume between 2 and 3 km beyond the observed values.

5.2 SEAC4RS field campaign

In the framework of the Studies of Emissions, Atmospheric Composition, Clouds and Climate Coupling by Regional Surveys (SEAC4RS) field campaign, the National Aeronautics and Space Administration (NASA) operates a DC-8 aircraft to sample the smoke plumes from fires in continental United States. Aerosol extinction was remotely sensed using a combined High

Spectral Resolution Lidar (HSRL, Hair et al., 2008) at 532nm and Ozone Differential Absorption Lidar at 290nm (DIAL, Browell et al., 1983). Measurements here focus on the aerosol measurements from the HSRL. These observations were used for the studies of the Rim Fire, which occurred in late August 2013 in California (Peterson et al., 2015) and were used to derive fire emissions using inversion techniques (Saide et al., 2015).

5   Here, we focus on a single flight from the DC-8 on 19th of August 2013. The track of the flight and the observed height of the mixed layer are shown in Figure 12. The cross-section of the aerosol extinction at 532nm observed by the DIAL-HSRL are presented in Figure 13a. Its most distinct feature is a series of elevated biomass burning aerosol layers between 4 and 6 km high, caused by large fires raging in the United States Pacific Northwest. Most of the aerosol burden lies above the top of the PBL, which was between 1 and 1.5 km.

10   The C-IFS forecasting system was run with biomass burning aerosols emissions prescribed at the surface (13b) and at the PRM mean height of maximum injection from GFAS (Figure 13c). The extinction resulting from the biomass burning is higher throughout the sampling regions when the injections heights were provided by GFAS as compared to emitting at the surface. The difference is especially important for altitudes between 2 and 6 km at 16:00 (35 °N), around 2 km between 18:00 and 19:00 (43-45 °N) and around 4 km between 20:00 and 22:00 (35-40 °N). The simulated values from C-IFS with injection

15   at surface underestimated aerosol extinction at altitudes higher than 3-4 km and sometimes overestimated extinction close to the surface. When using injection heights from GFAS, the smoke layer at higher altitudes is slightly better represented, but the overestimation close to the surface is also larger. The elevated layer of aerosols around 6 km is not captured by either simulation, which can be caused by errors either in the sources or in the transport and evolution of these smoke plumes.

6   Conclusions

20   Two existing algorithms estimating fire injection heights have been embedded into the GFAS system: the IS4FIRES parameterization and the Plume Rise Model. The new GFAS version provides daily global fire emissions and injection heights at a resolution of 0.1 °. It uses FRP from MODIS and atmospheric profiles from the operational ECMWF model as input. GFAS has been run for the period 2003-2014, and is now running in near real-time to provide biomass burning emissions for the C-IFS model.

25   The validation of the injection heights from GFAS against the MPHP2 dataset of plume heights observed by MISR show that both algorithms are suitable for plume height estimation, albeit with particular strengths in different respects: The IS4FIRES injection heights achieves better bias and RMSE scores globally and locally, while the PRM appears to represent large injection heights more accurately and to better reproduce the variability of injection heights. Inaccuracies in the input data obviously impact the scores. This is thought to be particular relevant in the cases of the planetary boundary layer height diagnostic from

30   ECMWF and a FRP underestimation for particularly large fires, where the MODIS Collection 5 products are known to have larger omission errors due to thick smoke being erroneously classified as cloud. To mitigate these errors, two datasets can also be used together in an optimal combination, with a larger variability than the IS4FIRES dataset and a smaller mean error and bias than the PRM dataset

The use of injection heights from GFAS for biomass burning emissions has been implemented in the global atmospheric composition model C-IFS. The scaling factors that are used in C-IFS for biomass-burning emissions of black carbon and organic matter were recomputed, with and without using injection heights; they showed little variation when the injection heights from GFAS are used. The new system was run and evaluated for two particular fire situation; the use of injection heights brought model profiles of aerosol extinction generally closer to observations compared to a simulation with emission injection prescribed at the surface. The forecast of high (i.e. above 4 km of altitude) plumes in particular seems to be improved by using injection heights in the C-IFS system.

The GFAS dataset of injection height information (and emission fluxes) is publicly available at the CAMS-GFAS dataserver at http://apps.ecmwf.int/datasets/data/cams-gfas. It can serve a variety of purposes, from the study of past fires to global atmospheric composition monitoring within the CAMS project for example. It can also provide input within the framework of model intercomparison projects such as the Aerosol Comparisons between Observations and Models (AEROCOM) project.

Acknowledgements. The authors wish to thank NASA for providing the MODIS data, and Charles Ichoku for providing Figure 2 reproduced from Ichoku and Ellison (2014).

The IS4FIRES algorithm was developed within the IS4FIRES project of the Academy of Finland.

Airborne data from the SAMBBA field campaign were obtained using the BAe-146-301 Atmospheric Research Aircraft (ARA) flown by Directflight Ltd and managed by the Facility for Airborne Atmospheric Measurements (FAAM), which is a joint entity of the Natural Environment Research Council (NERC) and the Met Office.

Support for the DIAL/HSRL operations and measurements during the SEAC4RS field campaign was provided by NASA Headquarter's Tropospheric Chemistry, Radiation Sciences, and Upper Atmospheric Research Programs. Support for the development and addition of the HSRL capability was provided by the NASA Airborne Instrument Technology Transition Program.

This research was supported by the EU Seventh Research Framework Programme (MACC-III project, contract number 283576).

7 Annex A: summary of differences between PRMv0 and PRMv2

Please refer to Freitas et al. (2007) and Freitas et al. (2010) for a detailed description of the basic PRMv0 equations. The main changes of PRMv2, as compared to PRMv0, are described in Paugam et al. (2015b). They consist of the addition of a mass conservation equation and a new scheme for plume entrainement and detrainement.

In PRMv0, plume entrainment is the sum of lateral entrainment and dynamical entrainemnt. Lateral entrainment is parameterized as a function of fire radius R and vertical velocity w (both prognostic variables of the model):

$$\gamma_{entr} = 2\frac{\alpha}{R}|w| \tag{2}$$

Where α is a fitting parameter. "Dynamic entrainment" is formulated as:

$$\delta_{entr} = 2\frac{1}{\pi R}(u_e - u) \tag{3}$$

Where u is the horizontal velocity at the center of the plume and u_e is the horizontal velocity of the environment. Plume detrainment is not taken into account.

In the PRMv2, entrainment and detrainment are parameterized as a function of buoyancy and vertical velocity following Pergaud et al. (2009), using a set of 4 parameters $C_\epsilon, C_\delta, C_{\epsilon,dyn}, C_{\delta,dyn}$, where the ϵ subscript stands for entrainment and δ for detrainment.

$$\epsilon = max(0, C_\epsilon \frac{B}{w^2}) + C_{\epsilon,dyn} \frac{1}{w}\frac{du}{dz} \tag{4}$$

$$\delta = max(0, C_\delta \frac{B}{w^2}) + C_{\epsilon,dyn} C_{\delta,dyn} \frac{1}{w}\frac{du}{dz} \tag{5}$$

Where B is the buoyancy. These 4 parameters, in addition to the β parameter that links Convective Heat Flux (CHF) and Fire Radiative Power (FRP), as well as another parameter used at initialization, need to be fitted using MISR observations. This is done in Paugam et al. (2015b) by using a selection of 38 particularly well-characterised plumes over North America from the MPHP dataset. These plumes satisfy all the following conditions:

– Fires are not over agricultural land,

– The mismatch between ECMWF winds and winds retrieved in MPHP is small,

– There is a limited number of fire clusters near the plume's origin,

– A plume is clearly and visibly observed,

– The plume is in a steady state, i.e. not in a development or dying out stage.

The parameter fitting procedure uses a Simulating Annealing algorithm and a Markov chain Monte Carlo uncertainty test. Table 1 summarizes the results of the optimization step for the six parameters. A value of 1 is used for the β parameter for simplicity's sake and because the confidence interval provided by the Monte Carlo uncertainty test was quite large for this particular parameter.

In PRMv2, mass conservation is described by the following equation:

$$\partial_t \zeta = -\partial_z(w\zeta) + w(\epsilon - \delta) \tag{6}$$

where $\zeta = \rho R^2$ can be interpreted as the mass per altitude meter, with ρ being the air density and R the radius of the plume.

Table 1. Optimal value of the input parameters of the PRMv2 model.

Parameter	Optimal value
α	0.039
C_ϵ	1.98
C_δ	-9.78
$C_{\epsilon,dyn}$	1.88
$C_{\delta,dyn}$	8.37
β	0.88

References

Achtemeier, G. L., Goodrick, S. A., Liu, Y., Garcia-Menendez, F., Hu, Y., and Odman, M. T.: Modeling smoke plume rise and dispersion from southern United States prescribed burns with daysmoke, Atmosphere, 2, 358-388, doi:10.3390/atmos2030358, 2011.

Ackerman, T. P., and O. B. Toon (1981), Absorption of visible radiation in atmosphere containing mixtures of absorbing and non-absorbing particles, Appl. Opt.,20, 3661-3667

Andela, N., Kaiser, J.W., Heil, A., Van Leeuwen, T.T., van der Werf, G.R., Wooster, M.J., Remy, S. and Schultz, M.G. : Assessment of the Global Fire Assimilation System (GFASv1), 2013. Available at https://gmes-atmosphere.eu/documents/maccii/deliverables/fir

Andela, N. and van der Werf, G.R.: Recent trends in african fires driven by cropland expansion and el nino to la nina transition. Nature Climate Change, 2014.

Andela, N., Kaiser, J. W., van der Werf, G. R., and Wooster, M. J.: New fire diurnal cycle characterizations to improve fire radiative energy assessments made from MODIS observations, Atmos. Chem. Phys., 15, 8831-8846, doi:10.5194/acp-15-8831-2015, 2015.

Angelo, C.: Amazon fire analysis hits new heights, Nature News, doi:10.1038/nature.2012.11467, 2012.

Andreae, M. O. and Merlet, P.: Emission of trace gases and aerosols from biomass burning, Global Biogeochem. Cy., 15, 955-966, 2001.

Andreae, M. O., Rosenfeld, D., Artaxo, P., Costa, A. A., Frank, G. P., Longo, K. M., and Silva-Dias, M. A. F.: Smoking rain clouds over the Amazon, Science, 303, 1337-1342, doi:10.1126/science.1092779, 2004

Benedetti, A., Morcrette, J.-J., Boucher, O., Dethof, A., Engelen, R.J., Fisher, M., Flentje, H., Huneeus, N., Jones, L., Kaiser, J.W., Kinne, S., Mangold, A., Razinger, M., Simmons, A.J. and Suttie, M., Aerosol analysis and forecast in the European Centre for Medium-Range Weather Forecasts Integrated Forecast System: 2. Data assimilation, J. Geophys. Res., 114, D13205, doi:10.1029/2008JD011115.

Boucher, O., Pham, M. and C. Venkataraman, Simulation of the atmospheric sulfur cycle in the LMD GCM: Model description, model evaluation, and global and European budgets, Note 23, 26 pp., Inst. Pierre-Simon Laplace, Paris, France, 2002.

Bowman, D. M. J. S., Balch, J. K., Artaxo, P., Bond, W. J., Carlson, J. M., Cochrane, M. A., D'Antonio, C. M., DeFries, R. S., Doyle, J. C., Harrison, S. P., Johnston, F. H., Keeley, J. E., Krawchuk, M. A., Kull, C. A., Marston, J. B., Moritz, M. A., Prentice, I. C., Roos, C. I., Scott, A. C., Swetnam, T. W., van der Werf, G. R., and Pyne, S. J.: Fire in the Earth System, Science, 324, 481-484, 2009.

Bond, T. C., Doherty, S. J., Fahey, D. W., Forster, P. M., Berntsen, T. K., Boucher, O., DeAngelo, B. J., Flanner, M. G., Ghan, S. J., Kärcher, B., Koch, D. and Kinne, S., Kondo, Y., Lohmann, U., Quinn, P. K., Sarofim, M. C., Schultz, M., Schulz, M., Venkataraman, C., Zhang, H., Zhang, S., Bellouin, N., Guttikunda, S., Hopke, P. K., Jacobson, M. Z., Kaiser, J. W., Klimont, Z., Schwarz, J. P., Shindell, D.,

Storelvmo, T., Warren, S. G. and Zender, C. S.: Bounding the role of black carbon in the climate system: A scientific assessment, Journal of Geophysical Research, 118, 1-173, 2013.

Browell, E. V., Carter, A. F., Shipley, S. T., Allen, R. J., Butler, C. F., Mayo, M. N., Siviter, J. H., and Hall, W. M.: NASA Multipurpose Airborne DIAL System and Measurements of Ozone and Aerosol Profiles, Appl Optics, 22, 522-534, 1983

5   Channan, S., K. Collins, and W. R. Emanuel.: Global mosaics of the standard MODIS land cover type data. University of Maryland and the Pacific Northwest National Laboratory, College Park, Maryland, USA, 2014.

Choi, J.-O. and Chung, C.-E.: Sensitivity of aerosol direct radiative forcing to aerosol vertical profile, Tellus B 2014, 66, 24376, doi:http://dx.doi.org/10.3402/tellusb.v66.24376, 2014.

Colarco, P.: The NASA GEOS-5 Aerosol Forecasting System, in: MACC Conference, Driebergen, The Netherlands, 2011.

10   Dahlkötter, F., Gysel, M., Sauer, F., Minikin, A., Baumann, R., Seifert, P., Ansmann, A., Fromm, M., Voigt, C. and Weinzierl, B.: The Pagami Creek smoke plume after long-range transport to the upper troposphere over Europe - aerosol properties and black carbon mixing state, Atmos. Chem. Phys. Discuss., 13, 28751-28818, 2013.

Damenov, A. and da Silva, A.: The Quick Fire Emissions Dataset (QFED) - Documentation of versions 2.1, 2.2 and 2.4, NASA Technical Report Series on Global Modeling and Data Assimilations, 32, 2013.

15   Dozier, J.: A method for satellite identification of surface temperature fields of subpixel resolution, Remote Sensing of Environment, 11, 221-229, doi:http://dx.doi.org/10.1016/0034-4257(81)90021-3, http://www.sciencedirect.com/science/article/pii/0034425781900213,1981.

Flemming, J., Huijnen, V., Arteta, J., Bechtold, P., Beljaars, A., Blechschmidt, A.-M., Diamantakis, M., Engelen, R. J., Gaudel, A., Inness, A., Jones, L., Josse, B., Katragkou, E., Marecal, V., Peuch, V.-H., Richter, A., Schultz, M. G., Stein, O., and Tsikerdekis, A.: Tropospheric chemistry in the Integrated Forecasting System of ECMWF, Geosci. Model Dev., 8, 975-1003, doi:10.5194/gmd-8-975-2015, 2015.

20   Using Ceilometers for the evaluation of MACC-II Modelled Aerosol Profiles, MACC-II Deliverable D_85.4, 2014.

Freeborn, P. H., Wooster, M. J., Roberts, G., Malamud, B. D., and Xu, W.: Development of a virtual active fire product for Africa through a synthesis of geostationary and polar orbiting satellite data, Remote Sens. Environ., 113, 1700-1711, 2009.

Freeborn, P.H. and Wooster, M.J., Addressing the spatiotemporal sampling design of MODIS to provide estimates of the fire radiative energy emitted from Africa, Remote Sensing of Environment, 115, 2, 475-489, 2011.

25   Freitas, S. R., Longo, K. M., Silva Dias, M. A. F., Silva Dias, P. L., Chatfield, R., Prins, E., Artaxo, P., Grell, G. A., and Recuero, F. S.: Monitoring the transport of biomass burning emissions in South America, Environ. Fluid Mech., 5, 135-167, 2005.

Freitas, S. R., Longo, K. M., and Andreae, M. O.: Impact of including the plume rise of vegetation fires in numerical simulations of associated atmospheric pollutants, Geophys. Res. Lett., 33,L17808, doi:10.1029/2006gl026608, 2006.

Freitas, S. R., Longo, K. M., Chatfield, R., Latham, D., Silva Dias, M. A. F., Andreae, M. O., Prins, E., Santos, J. C., Gielow, R., and Carvalho

30   Jr., J. A.: Including the sub-grid scale plume rise of vegetation fires in low resolution atmospheric transport models, Atmos. Chem. Phys., 7, 3385-3398, doi: 10.5194/acp-7-3385-2007

Freitas, S. R., Longo, K. M., Trentmann, J., and Latham, D.: Technical Note: Sensitivity of 1-D smoke plume rise models to the inclusion of environmental wind drag, Atmospheric Chemistry and Physics Discussions, 9, 14 713-14 733, 2010.

Fromm, M., Bevilacqua, R., Servranckx, R., Rosen, J., Thayer, J. P., Herman, J., and Larko, D.: Pyro-cumulonimbus injection of smoke to

35   the stratosphere: observations and impact of a super blowup in northwestern Canada on 3-4 August 1998, J. Geophys. Res.-Atmos., 110, D08205, doi: 10.1029/2004JD005350, 2005.

Fromm, M., Lindsey, D. T., Servranckx, R., Yue, G., Trickl, T., Sica, R., Doucet, P., and Godin-Beekmann, S.: The untold story of Pyrocumulonimbus, B. Am. Meteorol. Soc., 91, 1193-1209, doi:10.1175/2010BAMS3004.1, 2010

Giglio, L., MODIS Collection 4 Active Fire Product User's Guide Version 2.3, Science Systems and Applications, Inc, 2005.

Giglio, L., Csiszar, I., Justice, C.O. 2006. Global distribution and seasonality of active fires as observed with the Terra and Aqua MODIS sensors. Journal of Geophysical Research - Biogeosciences, Vol 111, G02016, doi:10.1029/2005JG000142.

Giglio, L., Descloitres, J., Justice, C.O., Kaufman, Y. 2003. An enhanced contextual fire detection algorithm for MODIS. Remote Sensing of Environment, 87:273-282.

Giglio, L.: Characterization of the tropical diurnal fire cycle using VIRS and MODIS observations, RSE, 108, 407-421, 2007.

Giglio, L., Randerson, J. T., van der Werf, G. R., Kasibhatla, P. S., Collatz, G. J., Morton, D. C., and DeFries, R. S.: Assessing variability and long-term trends in burned area by merging multiple satellite fire products, Biogeosciences, 7, 1171-1186, doi:10.5194/bg-7-1171-2010, 2010.

Giglio, L., J. T. Randerson, and G. R. van der Werf: Analysis of daily, monthly, and annual burned area using the fourth-generation global fire emissions database (GFED4) J. Geophys. Res. Biogeosci., 118, 317-328, doi:10.1002/jgrg.20042, 2013.

Hair, J. W., C. A. Hostetler, A. L. Cook, D. B. Harper, R. A. Ferrare, T. L. Mack, W. Welch, L. R. Izquierdo, and F. E. Hovis , 2008), Airborne high spectral resolution lidar for profiling aerosol optical properties, Appl. Opt., 47, 6734-6752, doi:10.1364/ao.47.006734.

Heald, C. L., Ridley, D. A., Kroll, J. H., Barrett, S. R. H., Cady-Pereira, K. E., Alvarado, M. J., and Holmes, C. D.: Contrasting the direct radiative effect and direct radiative forcing of aerosols, Atmos. Chem. Phys., 14, 5513-5527, doi:10.5194/acp-14-5513-2014, 2014.

Heil, A., Kaiser, J. W., van der Werf, G. R., Wooster, M. J., Schultz, M. G., and Dernier van der Gon, H.: Assessment of the Real-Time Fire Emissions (GFASv0) by MACC, Tech. Memo. 628, ECMWF, Reading, UK, 2010.

Hollingsworth, A., Engelen, R. J., Textor, C., Benedetti, A., Boucher, O., Chevallier, F., Dethof, A., Elbern, H., Eskes, H., Flemming, J., Granier, C., Kaiser, J. W., Morcrette, J.-J., Rayner, P., Peuch, V.-H., Rouil, L., Schultz, M. G., and Simmons, A. J.: Toward a Monitoring and Forecasting System For Atmospheric Composition: The GEMS Project, Bull. Am. Meteor. Soc., 89, 1147-1164, 2008.

C. Ichoku and Y. J. Kaufman. A method to derive smoke emission rates from MODIS fire radiative energy measurements. IEEE TGRS, 43(11):2636-2649, 2005.

Ichoku, C. and Ellison, L.: Global top-down smoke-aerosol emissions estimation using satellite fire radiative power measurements, Atmos. Chem. Phys., 14, 6643-6667, doi:10.5194/acp-14-6643-2014, 2014.

Inness, A., Baier, F., Benedetti, A., Bouarar, I., Chabrillat, S., Clark, H., Clerbaux, C., Coheur, P., Engelen, R. J., Errera, Q., Flemming, J., George, M., Granier, C., Hadji-Lazaro, J., Huijnen, V., Hurtmans, D., Jones, L., Kaiser, J. W., Kapsomenakis, J., Lefever, K., Leit~ao, J., Razinger, M., Richter, A., Schultz, M. G., Simmons, A. J., Suttie, M., Stein, O., Thépaut, J.-N., Thouret, V., Vrekoussis, M., Zerefos, C., and the MACC team: The MACC reanalysis: an 8-yr data set of atmospheric composition, Atmos. Chem. Phys. Discuss., 12, 31247-31347, doi:10.5194/acpd-12-31247-2012, 2012.

Inness, A., Benedetti, A., Flemming, J., Huijnen, V., Kaiser, J. W., Parrington, M., and Remy, S.: The ENSO signal in atmospheric composition fields: emission-driven versus dynamically induced changes, Atmos. Chem. Phys., 15, 9083-9097, doi:10.5194/acp-15-9083-2015, 2015.

Justice, C. O., Giglio, L., Korontzi, S., Owens, J., Morisette, J. T., Roy, D., Descloitres, J., Alleaume, S., Petitcolin, F., and Kaufman, Y.: The MODIS fire products, RSE, 83, 244-262, 2002.

Kahn, R. A., Li, W.-H., Moroney, C., Diner, D. J., Martonchik, J. V., and Fishbein, E.: Aerosol source plume physical characteristics from space-based multiangle imaging, J. Geophys. Res.-Atmos., 112, D11205, doi: 10.1029/2006JD007647

Kahn, R. A., Chen, Y., Nelson, D. L., Leung, F.-Y., Li, Q., Diner, D. J., and Logan, J. A.: Wildfire smoke injection heights: two perspectives from space, Geophys. Res. Lett., 35, L04809, doi:10.1029/2007GL032165, 2008

Kaiser, J.W., Andela, N., Atherton, J., de Jong, M., Heil, A., Paugam, R., Remy, S., Schultz, M.G., van der Werf, G.R., van Leeuwen, T.T. and Wooster, M.J. ; Recommended Fire Emission Service Enhancements, 2013. Available at https://gmes-atmosphere.eu/documents/maccii/deliverables/fir

Kaiser, J.W., Heil, A.,Andreae, M.O., Benedetti, A.,Chubarova, N.,Jones, L. ,Morcrette, J.-J.,Razinger, M., Schultz, M.G.,Suttie, M. and van der Werf, G.W.: Biomass burning emissions estimated with a global fire assimilation system based on observed fire radiative power, Biogeosciences, 9, 527-554, 2012

Kaiser, J. W., Suttie, M., Flemming, J., Morcrette, J.-J., Boucher, O. and Schultz, M. G.: Global Real-time Fire Emission Estimates Based on Space-borne Fire Radiative Power Observations, AIP Conf. Proc., 1100, 645–648, 2009.

Kessler, E.: On the distribution and continuity of water substance in atmospheric circulation models, Meteor. Monographs, 10, Am. Meteorol. Soc. Boston, MA, 1969.

Kolusu, S. R., Marsham, J. H., Mulcahy, J., Johnson, B., Dunning, C., Bush, M., and Spracklen, D. V.: Impacts of Amazonia biomass burning aerosols assessed from short-range weather forecasts, Atmos. Chem. Phys., 15, 12251-12266, doi:10.5194/acp-15-12251-2015, 2015.

Kouznetsov, R., Wood, C., Soares, J., Sofiev, M., Karppinen, A., and Fortelius, C.: Sodar verification for boundary-layer height diagnostics in meteorological models, in Proc. 16-th Int. Symp. for the Advancement of Boundary Layer Remote Sensing (P01-7, 1-4). Boulder, CO., PO1-7, 1-4, Boulder, CO, 2012.

Kukkonen, J., Nikmo, J., Sofiev, M., Riikonen, K., Petäjä, T., Virkkula, A., Levula, J., Schobesberger, S., and Webber, D. M.: Applicability of an integrated plume rise model for the dispersion from wildland fires, Geosci. Model Dev., 7, 2663-2681, doi:10.5194/gmd-7-2663-2014, 2014.

Latham, D.: PLUMP: A one-dimensional plume predictor and cloud model for fire and smoke managers, General Technical Report INT-GTR-314, Intermountain Research Station, USDA Forest Service, November, 1994

Marenco, F., Johnson, B., Langridge, J. M., Mulcahy, J., Benedetti, A., Remy, S., Jones, L., Szpek, K., Haywood, J., Longo, K., and Artaxo, P.: On the vertical distribution of smoke in the Amazonian atmosphere during the dry season, Atmos. Chem. Phys., 16, 2155-2174, doi:10.5194/acp-16-2155-2016, 2016.

Morcrette, J.-J., Boucher, O., Jones, L., Salmond, D., Bechtold, B., Beljaars, A., Benedetti, A., Bonet, A., Kaiser, J.W., Razinger, M., Schulz, M., Serrar, S., Simmons, A.J., Sofiev, M., Suttie, M., Tompkins, A.M. and Untch, A. , 2009), Aerosol analysis and forecast in the European Centre for Medium-Range Weather Forecasts Integrated Forecast System: Forward modeling, J. Geophys. Res., 114, D06206, doi:10.1029/2008JD011235.

Nelson, D. L., Chen, Y., Kahn, R. A., Diner, D. J., and Mazzoni, D.: Example applications of the MISR INteractive eXplorer (MINX) software tool to wildfire smoke plume analyses, Proc. SPIE, 7089, 708909-708909-11, doi:10.1117/12.795087, 2008.

Nelson, D., Garay, M., Kahn, R., and Dunst, B.: Stereoscopic Height and Wind Retrievals for Aerosol Plumes with the MISR INteractive eXplorer (MINX), Remote Sens., 5, 4593-4628, doi:10.3390/rs5094593, 2013.

Palm, S. P., A. Benedetti, and J. Spinhirne: Validation of ECMWF global forecast model parameters using GLAS atmospheric channel measurements, Geophys. Res. Lett., 32, L22S09, doi:10.1029/2005GL023535, 2005.

Paugam, R., Wooster, M., Freitas, S. R., and Val Martin, M.: A review of approaches to estimate wildfire plume injection height within large scale atmospheric chemical transport models Part 1, Atmos. Chem. Phys. Discuss., 15, 9767-9813, doi:10.5194/acpd-15-9767-2015, 2015.

Paugam, R., Wooster, M., Atherton, J., Freitas, S. R., Schultz, M. G., and Kaiser, J. W.: Development and optimization of a wildfire plume rise model based on remote sensing data inputs Part 2, Atmos. Chem. Phys. Discuss., 15, 9815-9895, doi:10.5194/acpd-15-9815-2015, 2015.

Pergaud, J., Masson, V., Malardel, S., and Couvreux, F.: A parameterization of dry thermals and shallow cumuli for mesoscale numerical weather prediction, Bound.-Lay. Meteorol., 132, 83-106, 2009. 9826, 9847, 9857, 9858

Peterson, D.A., Hyer, E.J., Campbell, J.R., Fromm, M.D., Hair, J.W., Butler, C.F. , and Fenn, M.A.: The 2013 Rim Fire: Implications for Predicting Extreme Fire Spread, Pyroconvection, and Smoke Emissions. Bull. Amer. Meteor. Soc., 96, 229-247, 2015.

Peuch, V.-H. and Engelen, R.J.: Towards and operational GMES Atmosphere Monitoring Service, ECMWF Newsletter No. 132, 20-25, 2012.

Reddy, M. S., Boucher, O., Bellouin, N., Schulz, M., Balkanski, Y., Dufresne J.-L. and M. Pham, Estimates of global multicomponent aerosol optical depth and direct radiative perturbation in the Laboratoire de Meteorologie Dynamique general circulation model, J. Geophys. Res., 110, D10S16, 2005.

Reid, J. S., Hyer, E. J., Prins, E. M., Westphal, D. L., Zhang, J., Wang, J., Christopher, S. A., Curtis, C. A., Schmidt, C. C., Eleuterio, D. P., Richardson, K. A., and Hoffman, J. P.: Global Monitoring and Forecasting of Biomass-Burning Smoke: Description of and Lessons from the Fire Locating and Modeling of Burning Emissions (FLAMBE) Program, IEEE J. Selected Topics Appl. Earth Observations and Remote Sens., 2, 144-162, 2009.

Remy, S. and Kaiser, J. W.: Daily global fire radiative power fields estimation from one or two MODIS instruments, Atmos. Chem. Phys., 14, 13377-13390, doi:10.5194/acp-14-13377-2014, 2014.

Roberts, G., Wooster, M J and Lagoudakis, E.: Annual and diurnal african biomass burning temporal dynamics, Biogeosciences, 6, 849-866, 2009.

Rosário, N. E., Longo, K. M., Freitas, S. R., Yamasoe, M. A., and Fonseca, R. M.: Modeling the South American regional smoke plume: aerosol optical depth variability and surface short-wave flux perturbation, Atmos. Chem. Phys., 13, 2923-2938, doi:10.5194/acp-13-2923-2013, 2013.

Saide, P. E., D. A. Peterson, A.da Silva, B. Anderson, L. D. Ziemba, G. Diskin, G. Sachse, J. Hair, C. Butler, M. Fenn, J. L. Jimenez, P. Campuzano-Jost, A. E. Perring, J. P. Schwarz, M. Z. Markovic, P. Russell, J. Redemann, Y. Shinozuka, D. G. Streets, F. Yan, J. Dibb, R. Yokelson, O. B. Toon, E. Hyer, and G. R. Carmichael: Revealing important nocturnal and day-to-day variations in fire smoke emissions through a multiplatform inversion. Geophys. Res. Lett., 42, 3609-3618, doi: 10.1002/2015GL063737, 2015.

Schroeder, W., Ellicott, E., Ichoku, C., Ellison, L., Dickinson, M. B., Ottmar, R. D., Clements, C., Hall, D., Ambrosia, V., and Kremens, R.: Integrated active fire retrievals and biomass burning emissions using complementary near-coincident ground, airborne and spaceborne sensor data, Remote Sens. Environ., 140, 719-730, doi:10.1016/j.rse.2013.10.010, 2014.

Simpson, J. and Wiggert, V.: Models of precipitating cumulus towers., Mon. Wea. Rev., 97, 471489, 1969.

Sofiev, M., Siljamo, P., Valkama, I., Ilvonen, M., and Kukkonen, J.: A dispersion modeling system SILAM and its evaluation against ETEX data, Atmos. Environ., 40, 674-685, doi:10.1016/j.atmosenv.2005.09.069, 2006.

Sofiev, M., Vankevich, R., Lotjonen, M., Prank, M., Petukhov, V., Ermakova, T., Koskinen, J., and Kukkonen, J.: An operational system for the assimilation of the satellite information on wild-land fires for the needs of air quality modeling and forecasting, Atmos. Chem. Phys., 9, 6833-6847, doi:10.5194/acp-9-6833-2009, 2009.

Sofiev, M., Ermakova, T., and Vankevich, R.: Evaluation of the smoke-injection height from wild-land fires using remote-sensing data, Atmos. Chem. Phys., 12, 1995-2006, doi:10.5194/acp-12-1995-2012, 2012.

Sofiev, M., Vankevich, R., Ermakova, T., and Hakkarainen, J.: Global mapping of maximum emission heights and resulting vertical profiles of wildfire emissions, Atmos. Chem. Phys., 13, 7039-7052, doi:10.5194/acp-13-7039-2013, 2013.

Strada, S., Freitas, S. R., Mari, C., Longo, K. M., and Paugam, R.: One-dimensional simulation of fire injection heights in contrasted meteorological scenarios with PRM and Meso-NH models, Geosci. Model Dev. Discuss., 6, 721-790, doi:10.5194/gmdd-6-721-2013, 2013.

Textor, C., Schulz, M., Guibert, S., Kinne, S., Balkanski, Y., Bauer, S., Berntsen, T., Berglen, T., Boucher, O., Chin, M., Dentener, F., Diehl, T., Easter, R., Feichter, H., Fillmore, D., Ghan, S., Ginoux, P., Gong, S., Grini, A., Hendricks, J., Horowitz, L., Huang, P., Isaksen, I., Iversen, I., Kloster, S., Koch, D., Kirkev ag, A., Kristjansson, J. E., Krol, M., Lauer, A., Lamarque, J. F., Liu, X., Montanaro, V., Myhre, G., Penner, J., Pitari, G., Reddy, S., Seland, O., Stier, P., Takemura, T., and Tie, X.: Analysis and quantification of the diversities of aerosol life cycles within AeroCom, Atmos. Chem. Phys., 6, 1777-1813, 2006.

Tosca, M. G., J. T. Randerson, C. S. Zender, D. L. Nelson, D. J. Diner, and J. A. Logan: Dynamics of fire plumes and smoke clouds associated with peat and deforestation fires in Indonesia, J. Geophys. Res., 116, D08207, doi:10.1029/2010JD015148, 2011.

Troen, I and Mahrt, L.: A simple model of the atmospheric boundary layer; sensitivity to surface evaporation. Boundary-Layer Meteorol., 37, 129-148, 1986.

Twomey, S.: The influence of pollution on the shortwave albedo of clouds, J. Atmos. Sci., 34, 1149-1152, doi:10.1175/1520-0469, 1977)034<1149:TIOPOT>2.0.CO;2, 1977.

Val Martin, M., Logan, J. A., Kahn, R. A., Leung, F.-Y., Nelson, D. L., and Diner, D. J.: Smoke injection heights from fires in North America: analysis of 5 years of satellite observations, Atmos. Chem. Phys., 10, 1491-1510, doi: 10.5194/acp-10-1491-2010, 2010.

Val Martin, M., Kahn, R. A., Logan, J. A., Paugam, R., Wooster, M., and Ichoku, C.: Space-based observational constraints for 1-D fire smoke plume-rise models, J. Geophys. Res., 117, D22204, doi:10.1029/2012JD018370, 2012.

van der Werf, G. R., Randerson, J. T., Giglio, L., Collatz, G. J., Mu, M., Kasibhatla, P. S., Morton, D. C., DeFries, R. S., Jin, Y., and van Leeuwen, T. T.: Global fire emissions and the contribution of deforestation, savanna, forest, agricultural, and peat fires , 1997-2009), Atmos. Chem. Phys., 10, 11707-11735, doi:10.5194/acp-10-11707-2010, 2010.

Veira, A., Kloster, S., Wilkenskjeld, S., and Remy, S.: Fire emission heights in the climate system Part 1: Global plume height patterns simulated by ECHAM6-HAM2, Atmos. Chem. Phys., 15, 7155-7171, doi:10.5194/acp-15-7155-2015, 2015.

Veira, A., Kloster, S., Schutgens, N. A. J., and Kaiser, J. W.: Fire emission heights in the climate system Part 2: Impact on transport, black carbon concentrations and radiation, Atmos. Chem. Phys., 15, 2015.

Wiedinmyer, C., Akagi, S. K., Yokelson, R. J., Emmons, L. K., Al-Saadi, J. A., Orlando, J. J. and Soja, A. J.: The Fire INventory from NCAR (FINN); a high resolution global model to estimate the emissions from open burning, Geosci. Model Dev, 4, 625-641, 2011.

Wiedinmyer, C.: Atmospheric chemistry: Breathing easier in the Amazon, Nature Geoscience, 8, 751-752, doi:10.1038/ngeo2550, 2015.

Wooster, M. J., Roberts, G., Perry, G. L. W., and Kaufman, Y. J.: Retrieval of biomass combustion rates and totals from fire radiative power observations: FRP derivation and calibration relationships between biomass consumption and fire radiative energy release, J. Geophys. Res., 110, D24311, 2005.
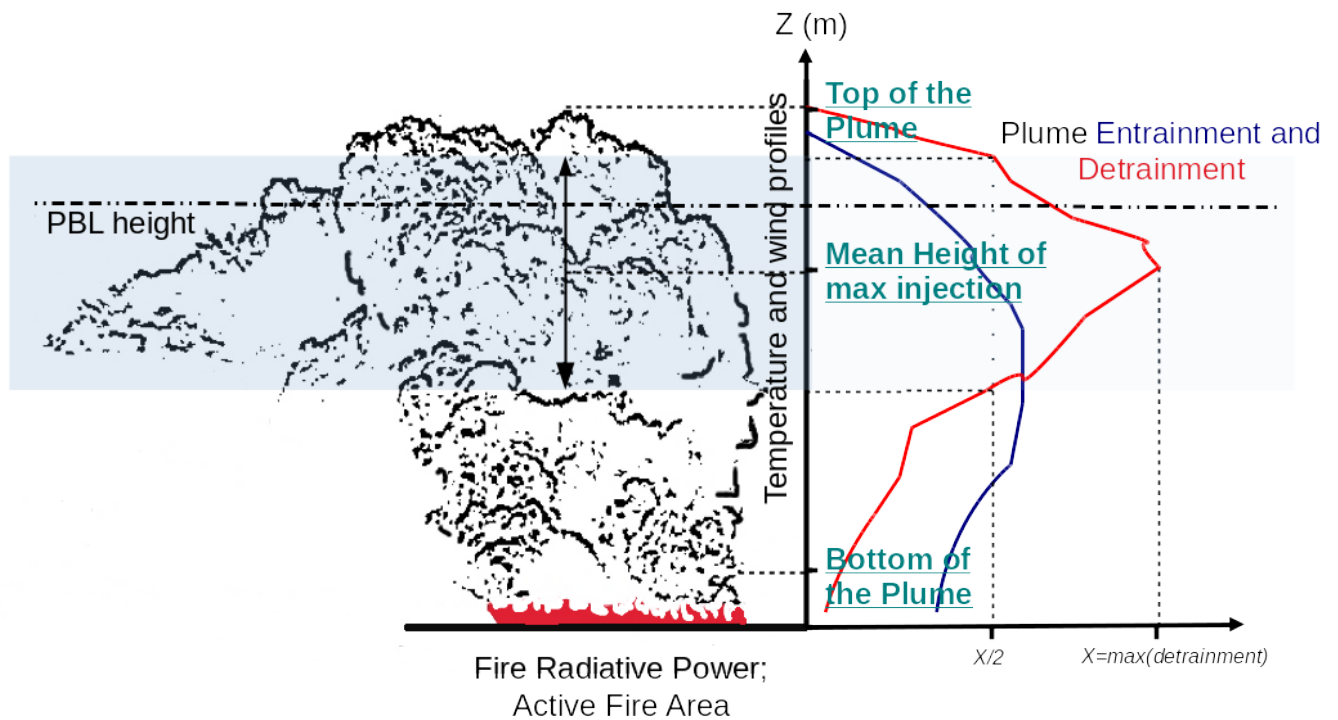
Figure 1. Schematic of an algorithm estimating plume injection height parameters. The fire input (Fire Radiative Power and fire area) and the environmental input (temperature and wind profiles) are shown, as well as the possible output of the model: detrainment and entrainment profiles, with the derived quantities (bottom of the plume, top of the plume, mean height of maximum injection), or injection height, usually defined as the top of the plume.
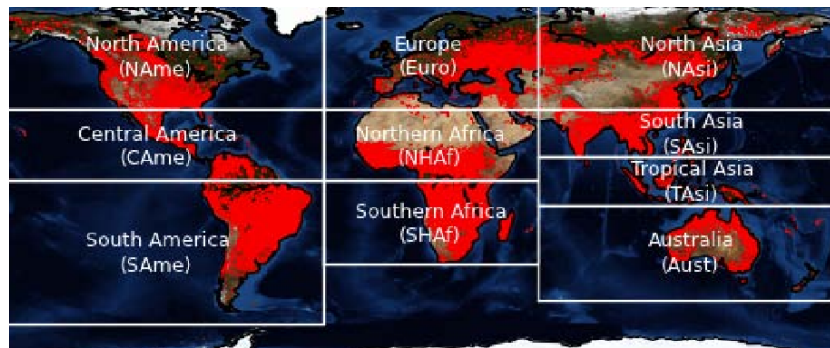
Figure 2. Regions of interest as defined in Kaiser et al. (2012).
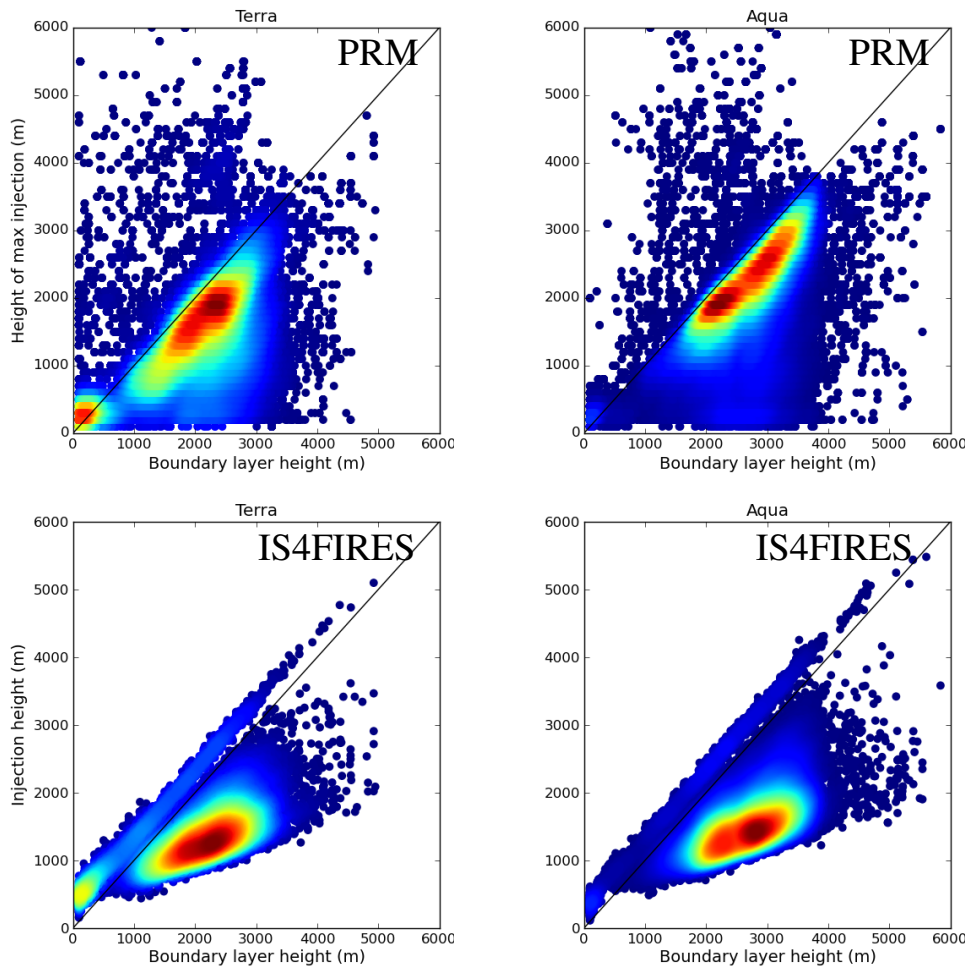
Figure 3. Comparison of the ECMWF boundary layer height diagnostic against raw height of maximum injection from the PRM (top) and from the IS4FIRES algorithm (middle) for the 1/6/2013 - 1/8/2013 period. Bottom, comparison of the raw height of maximum injection from the PRM against the injection height from IS4FIRES. Observations used are from Terra (left) and Aqua (right).
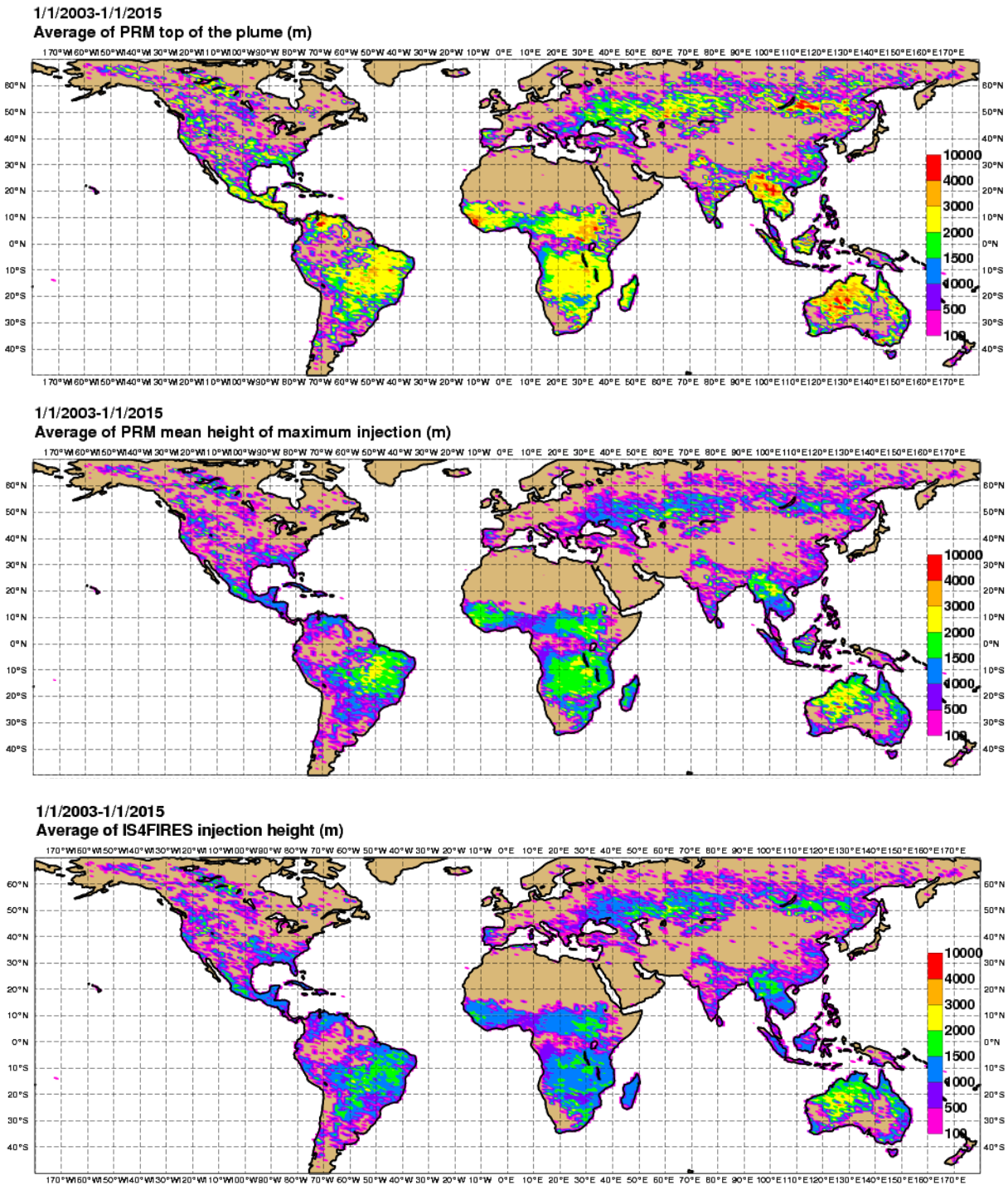
Figure 4. Global average for the 1/1/2003 - 1/1/2015 period of daily injection heights from GFAS. Top of the plume (top) and mean height of maximum injection (middle) from the PRM, and injection height estimated with the IS4FIRES parameterization (bottom). The averages were computed taking into account only non-null values.
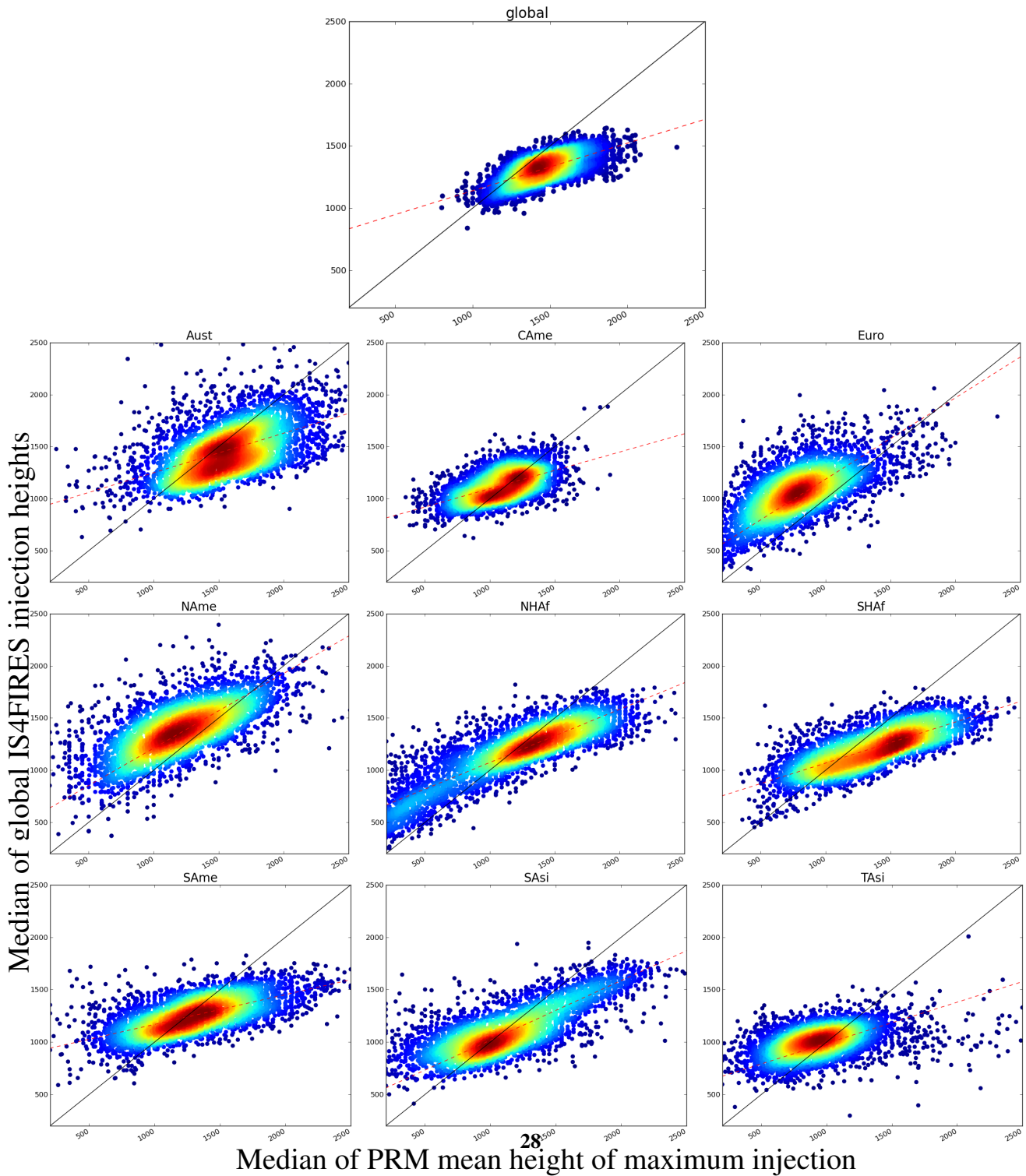
Figure 5. Density plots of global and regional comparison of the median of global IS4FIRES injection height against the median of the
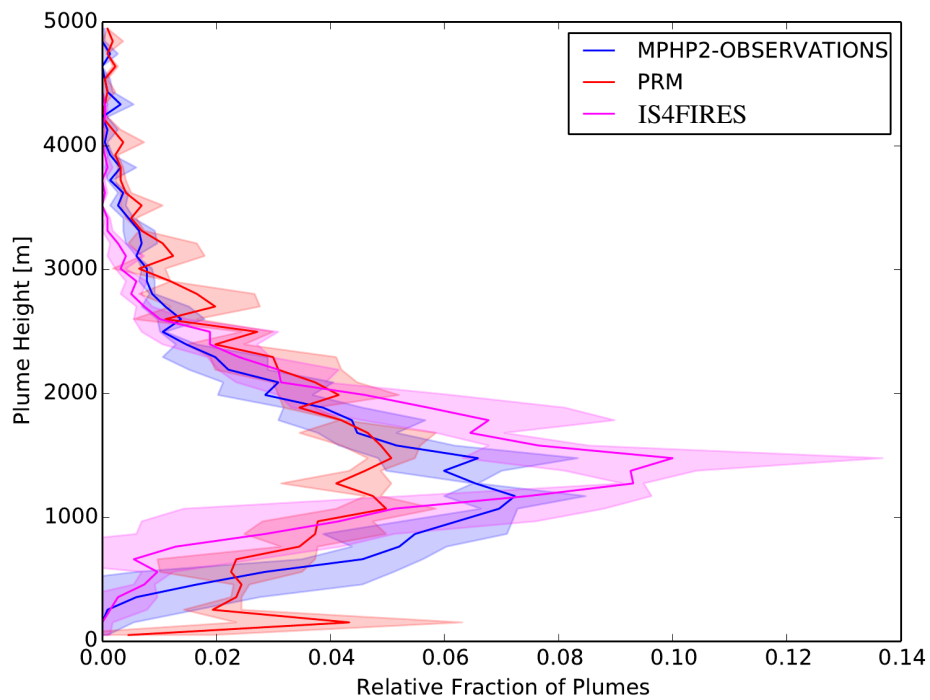
Figure 6. Global distribution of injection height from IS4FIRES and mean height of maximum injection from the PRM (for fires with MPHP2 observations),and of MPHP2 observations for 2008. Shading represents uncertainties of 200 m in the plume height observations and parametrizations. The sum over the vertical of the relative fractions is 1 for all curves.
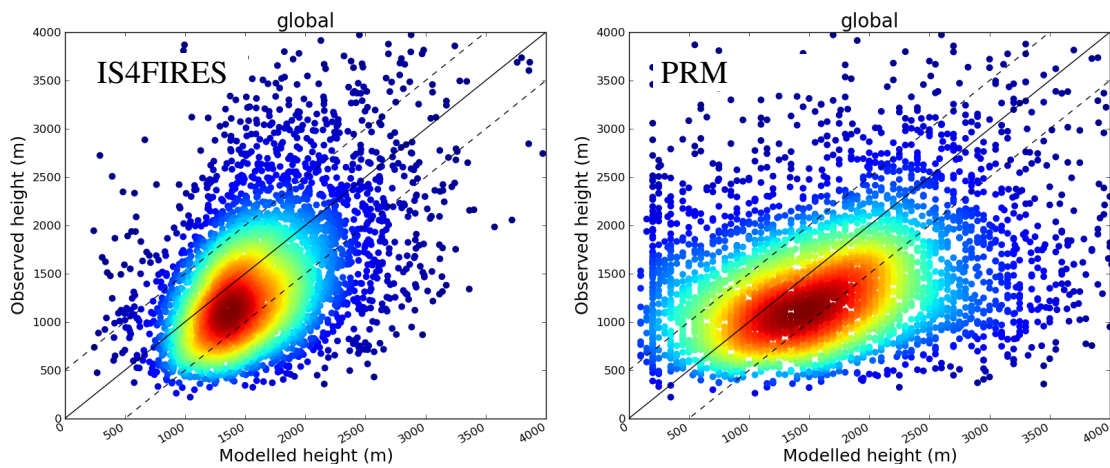
Figure 7. Density plots of global comparison of the MPHP2 observations of plume height in 2008 against the IS4FIRES (left) and the PRM (right) injection heights of GFAS. MPHP2 observations with "good" and "fair" quality flags were used. The dashed lines delineate the area in which the GFAS injection heights are within 500 m of observations.
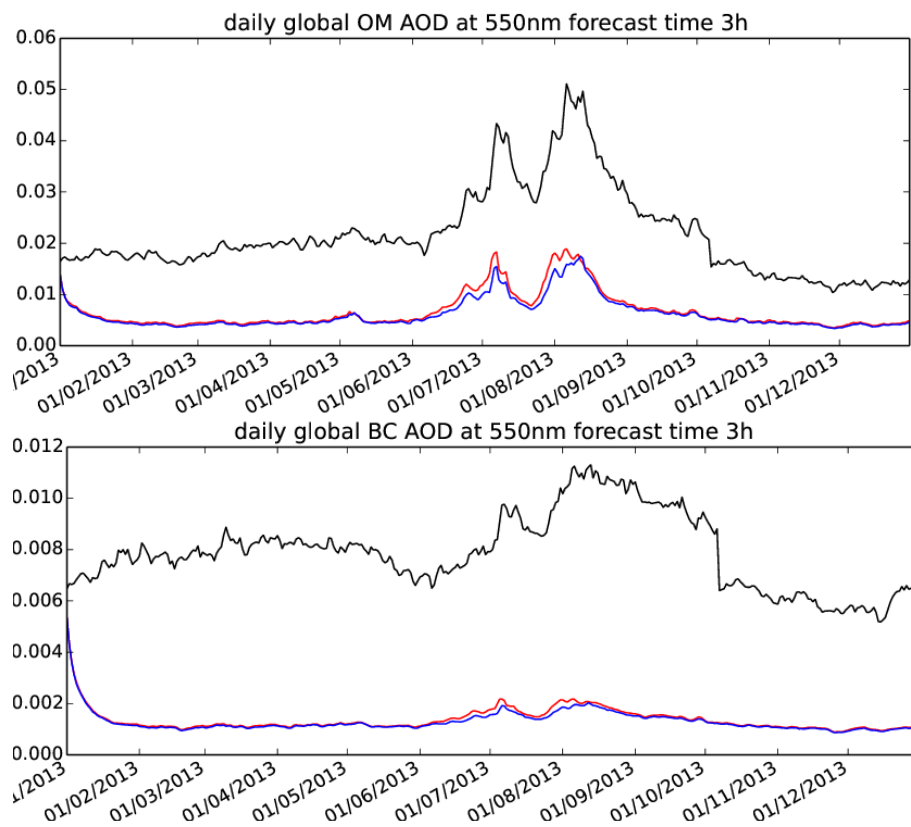
Figure 8. Global optical depth at 550 nm of Organic Matter (OM) aerosol (top) and Black Carbon (BC,bottom) for the year 2013, simulated by C-IFS. The simulation with data assimilation is in black (biomass burning emissions are prescribed at the surface); without assimilation and with biomass burning aerosol emissions prescribed at the surface is in blue; at the PRM injection height in red.
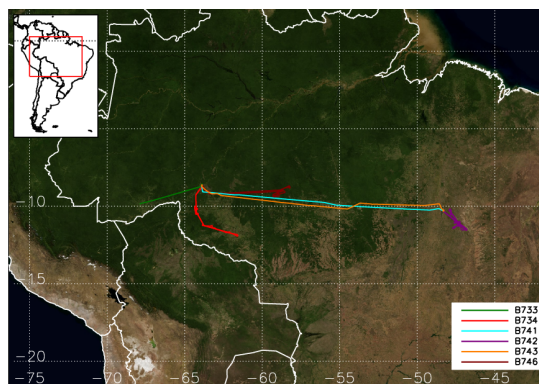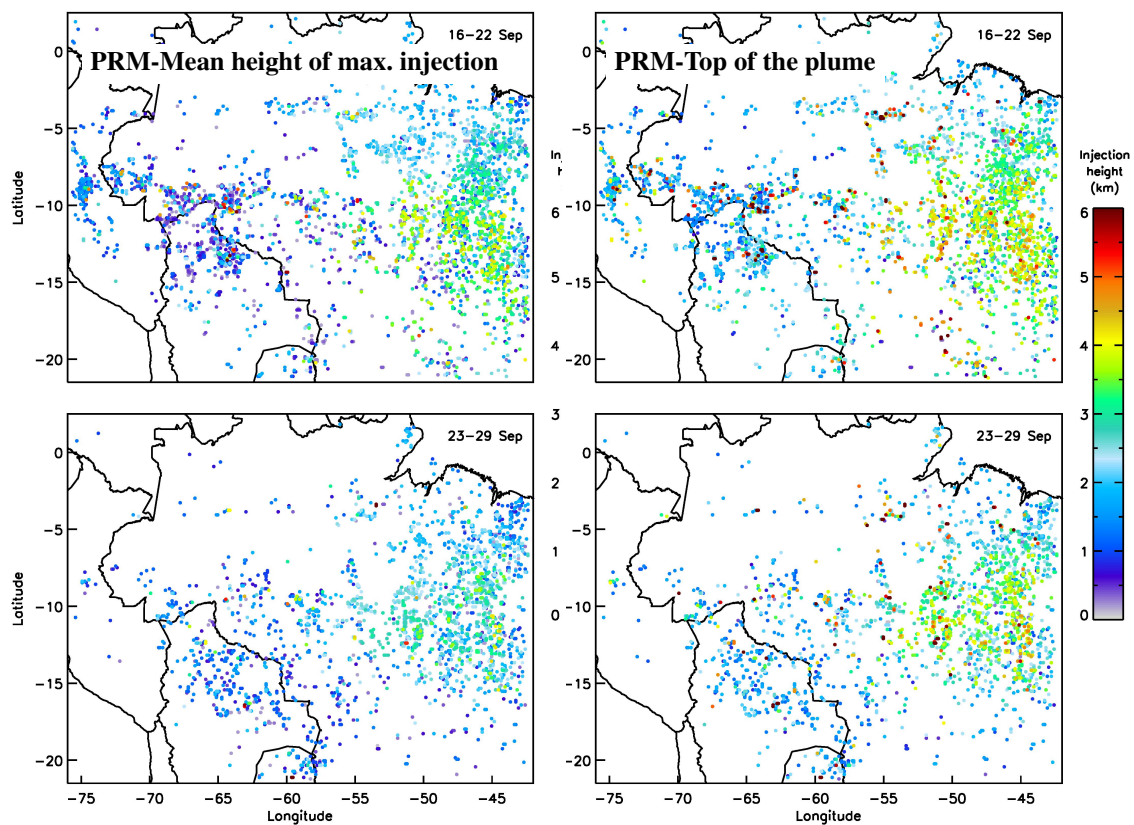
Figure 9. Left, PRM mean height of maximum injection from GFAS, accumulated values from 16-22 September 2012 (top) and 23-29 September 2012 (middle). Right, PRM top of the plume from GFAS, accumulated values from 16-22 September 2012 (top) and 23-29 September 2012 (middle). At the bottom, ground tracks of the six research flights of the SAMBBA field campaign listed in Table 5.
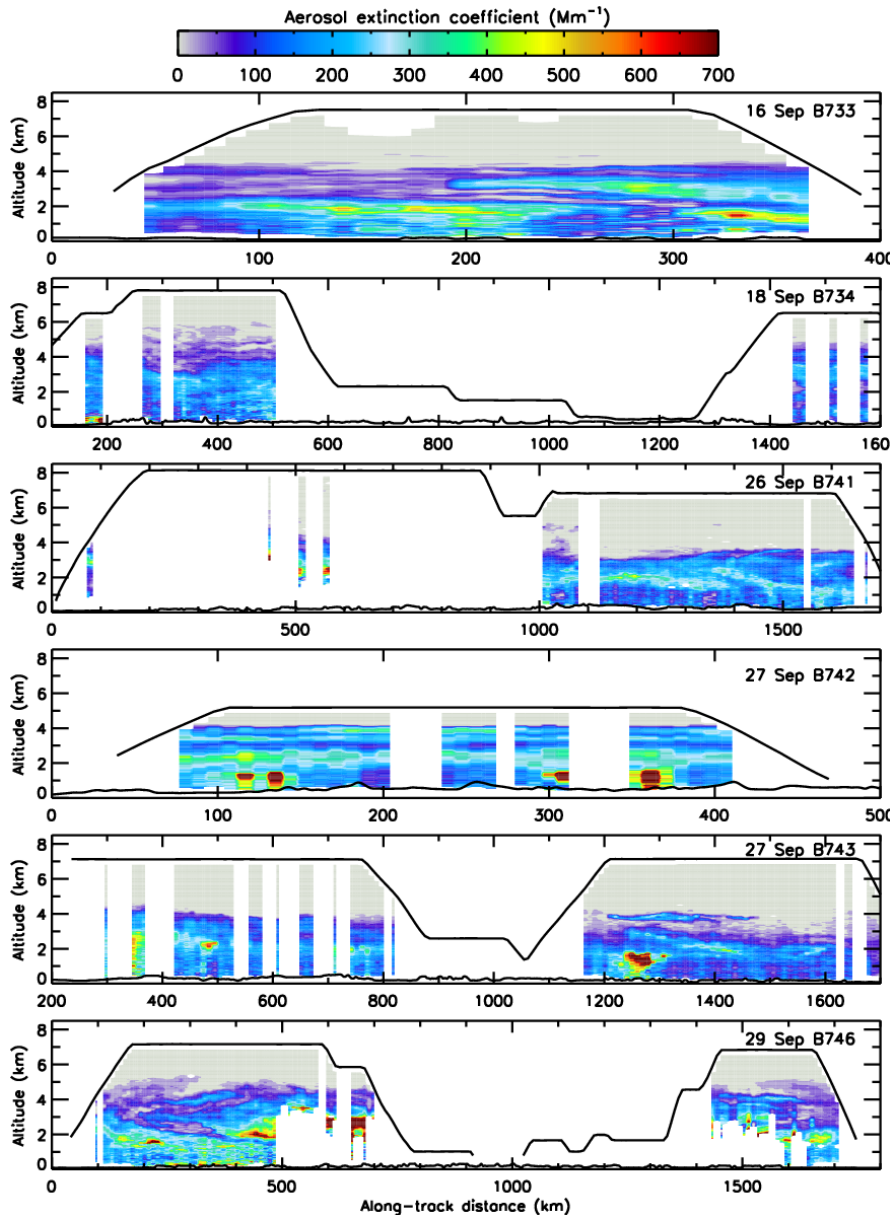
Figure 10. Cross-sections of the aerosol extinction at 355nm coefficient determined from the lidar for the six research flights with a 1-minute integration time. The black lines indicate the aircraft altitude and the surface elevation from a digital elevation model, respectively.
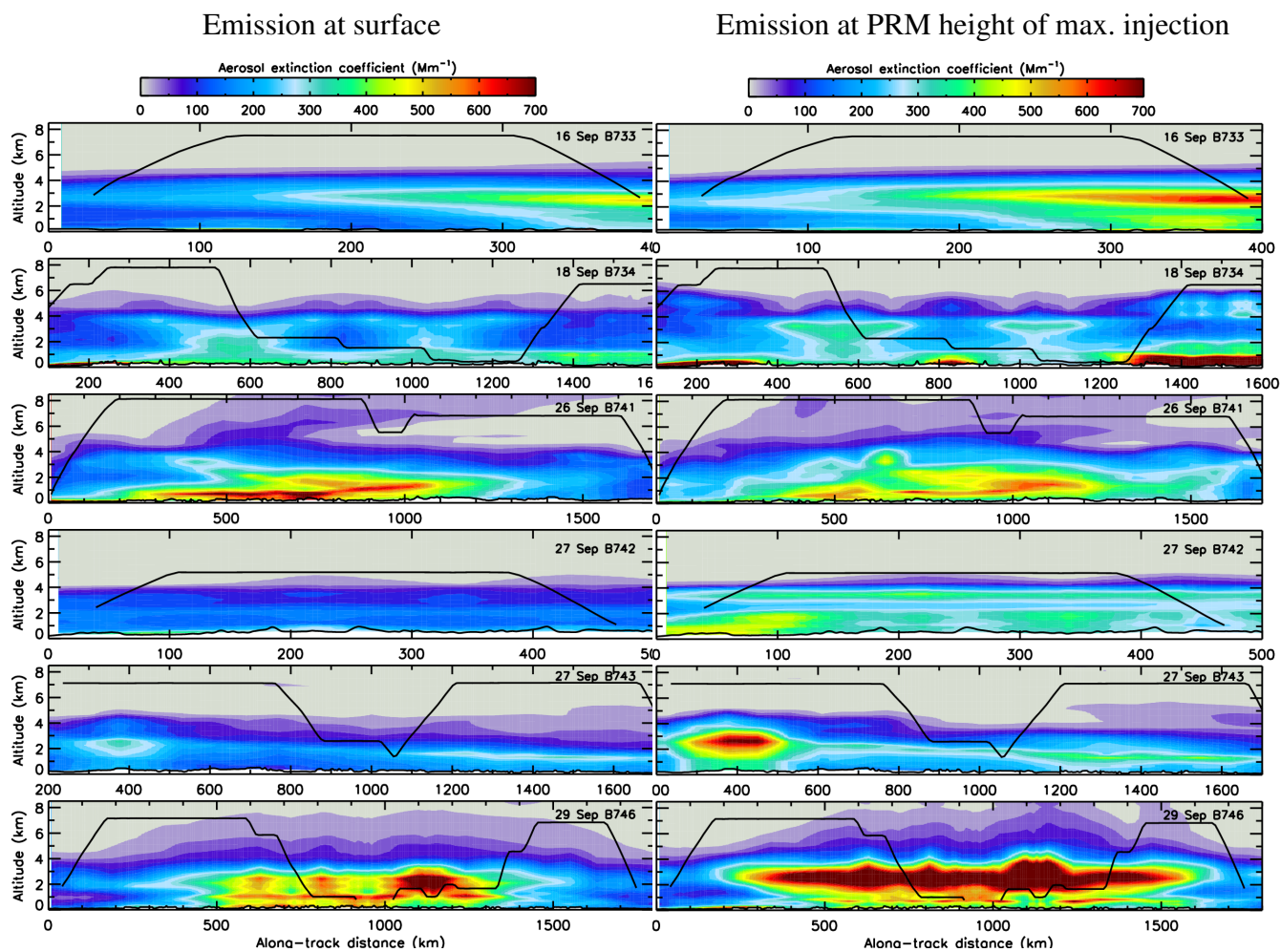
Figure 11. Cross-sections of the aerosol extinction coefficient at 532nm estimated from the C-IFS along the tracks of the six research flights. Biomass burning aerosols are emitted at the surface (left) and at the PRM mean height of maximum injection provided by GFAS (right).
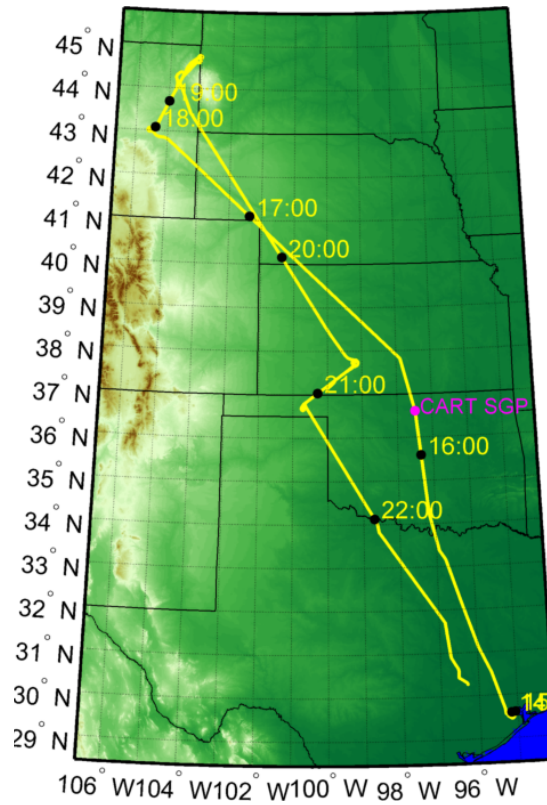
Figure 12. Ground tracks for the 19th August 2013 research flight of the SEAC4RS field campaign, in southern U.S.A.. CART SGP stands for the Cloud and Radiation Testbed (CART) Southern Great Plains (SGP) site.
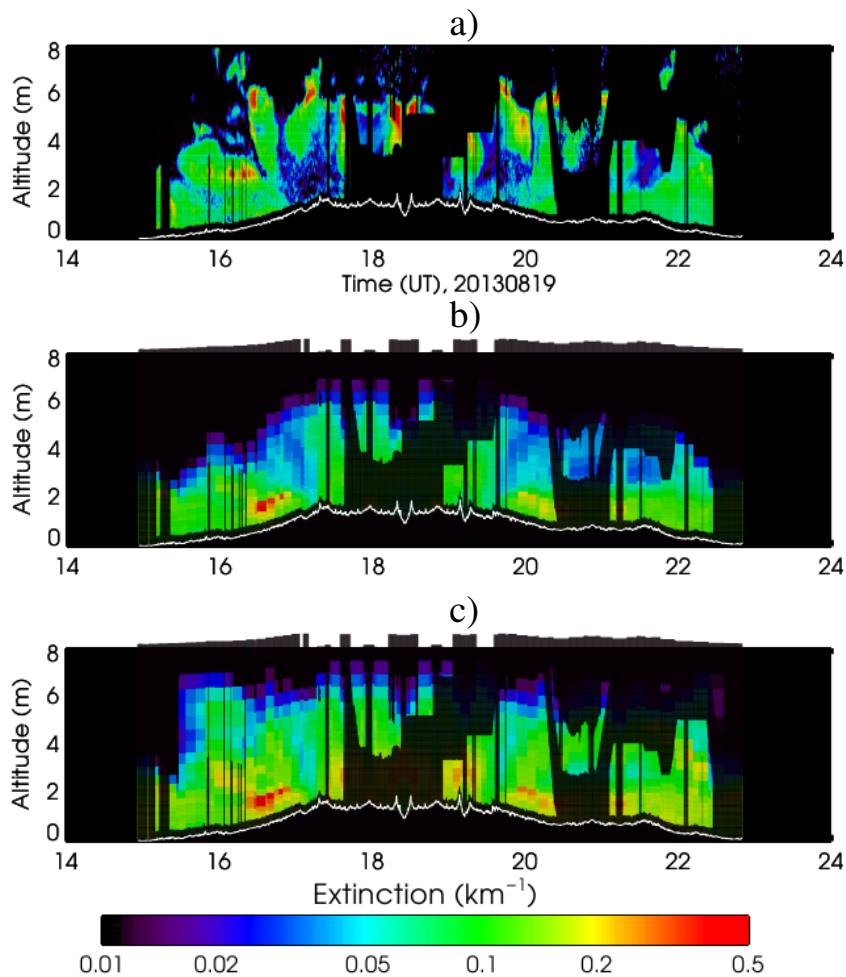
Figure 13. Cross-sections of the aerosol extinction at 532nm; a), observed along the tracks of the research flights of SEAC4RS of 19/8/2013; b) C-IFS forecast with biomass burning aerosols emitted at surface and c) at the PRM mean height of maximum injection provided by GFAS.

Table 2. Statistical analysis of the IS4FIRES and the PRM plume height in GFAS over the period 1/1/2003 - 1/1/2015, together with the mean of the PBL height diagnostic from the operational ECMWF model at the points where there were fires. All values are in meters and computed for the same fires. Only the non-null values were used in the computation of the statistics. "IS4" stands for "IS4FIRES Parameterization", "PRM" for "Plume Rise Model"

Region name	mean-IS4/PRM	mean PBL h.	1st decile-IS4/PRM	5th decile-IS4/PRM	9th decile-IS4/PRM
Global	1377 / 1536	1634	792 / 431	1316 / 1460	2026 / 2680
Australia	1522 / 1570	1955	889 / 465	1465 / 1567	2218 / 2616
Central America	1173 / 1164	1620	818 / 388	1129 / 1092	1586 / 1963
Europe	1021 / 836	1585	591 / 245	985 / 740	1490 / 1550
North America	1361 / 1193	1611	858 / 396	1398 / 1138	1928 / 2018
North Asia	1179 / 1022	1493	741 / 320	1144 / 966	1656 / 1768
N. Hem. Africa	1168 / 1309	2054	685 / 425	1167 / 1184	1771 / 2333
S. Hem. Africa	1272 / 1424	2321	801 / 529	1209 / 1359	1814 / 2364
South America	1316 / 1375	1809	829 / 371	1255 / 1305	1882 / 2406
South Asia	1105 / 1147	1591	788 / 466	1066 / 1096	1472 / 1871
Tropical Asia	983 / 1092	1079	697 / 404	954 / 916	1306 / 1970

Table 3. Scores of IS4FIRES / PRM plume height against the MPHP2 dataset for the year 2008, for each regions defined in figure 1. The "% inside" score correspond to the relative fraction of estimated plumes that are within 500 m of the MPHP2 observations

Region name	sample size	RMSE-IS4/PRM (m)	bias-IS4/PRM (m)	mean-IS4/PRM (m)	R-IS4/PRM	% inside-IS4/PRM
Global	4182	533 / 955	144 / 239	1619 / 1714	0.45 / 0.31	57 / 44
Australia	306	652 / 863	120 / 186	1555 / 1620	0.55 / 0.44	57 / 50
Central America	151	426 / 684	117 / 43	1453 / 1380	0.22 / 0.10	63 / 50
North America	251	632 / 1071	-69 / -110	1832 / 1791	0.59 / 0.37	55 / 42
Europe	196	489 / 879	-133 / -96	1596 / 1634	0.41 / 0.33	53 / 45
North Asia	997	497 / 852	-13 / -73	1626 / 1567	0.47 / 0.32	64 / 49
North Hem. Africa	836	486 / 1073	180 / 401	1616 / 1836	0.39 / 0.40	57 / 44
South Hem. Africa	825	631 / 1010	375 / 584	1668 / 1876	0.42 / 0.38	54 / 40
South America	520	556 / 1108	273 / 424	1585 / 1736	0.47 / 0.30	48 / 61
South Asia	90	537 / 969	26 / 63	1307 / 1339	0.46 / 0.40	65 / 61
Tropical Asia	11	297 / 1670	-182 / 923	1357 / 2462	0.14 / 0.13	64 / 18

Table 4. Scores of IS4FIRES / PRM plume height against the MPHP2 dataset for the year 2008, for each IGBP biome type. The "% inside" score correspond to the relative fraction of estimated plumes that are within 500 m of the MPHP2 observations

IGBP Biome type	sample size	RMSE-IS4/PRM (m)	bias-IS4/PRM (m)	mean-IS4/PRM (m)	R-IS4/PRM	% inside-IS4/PRM
All	4182	533 / 955	144 / 239	1619 / 1714	0.45 / 0.31	57 / 44
Evergreen broad-leaf	248	521 / 1222	289 / 664	1475 / 1850	0.42 / 0.29	51 / 40
Deciduous needle-leaf	229	428 / 705	-87 / 17	1533 / 1637	0.47 / 0.21	65 / 48
Mixed forest	206	503 / 816	-26 / -190	1557 / 1394	0.40 / 0.21	62 / 51
Open shrublands	318	659 / 961	61 / 114	1725 / 1779	0.54 / 0.40	58 / 48
Woody savannas	1040	566 / 942	272 / 403	1596 / 1833	0.40 / 0.37	58 / 43
Savannas	1058	524 / 1063	180 / 376	1636 / 1833	0.41 / 0.37	56 / 43
Grasslands	316	533 / 953	47 / -67	1811 / 1697	0.35 / 0.29	51 / 42
Croplands	239	472 / 851	73 / 65	1566 / 1558	0.50 / 0.39	56 / 50
Cropland / veg. mosaic	327	444 / 851	117 / 65	1511 / 1525	0.40 / 0.24	64 / 48

Table 5. Research flights of the SAMBBA field campaign considered in this article. Time is UTC.

Flight	Date	Takeoff	Landing	Latitude	Longitude
B733	16 Sep	Rio Branco, 13:51	Porto Velho, 14:45	8.9-9.8S	64.5-67.6W
B734	18 Sep	Porto Velho, 12:05	Porto Velho, 16:01	8.9-11.9S	61.6-64.4W
B741	26 Sep	Porto Velho, 12:53	Palmas, 16:08	8.8-10.2S	48.7-63.9W
B742	27 Sep	Palmas, 12:52	Palmas, 16:17	10.2-11.5S	46.8-48.1W
B743	27 Sep	Palmas, 18:08	Porto Velho, 21:34	9.0-10.2S	48.4-63.6W
B746	29 Sep	Porto Velho, 12:54	Porto Velho, 16:38	8.7-9.4S	58.2-63.7W